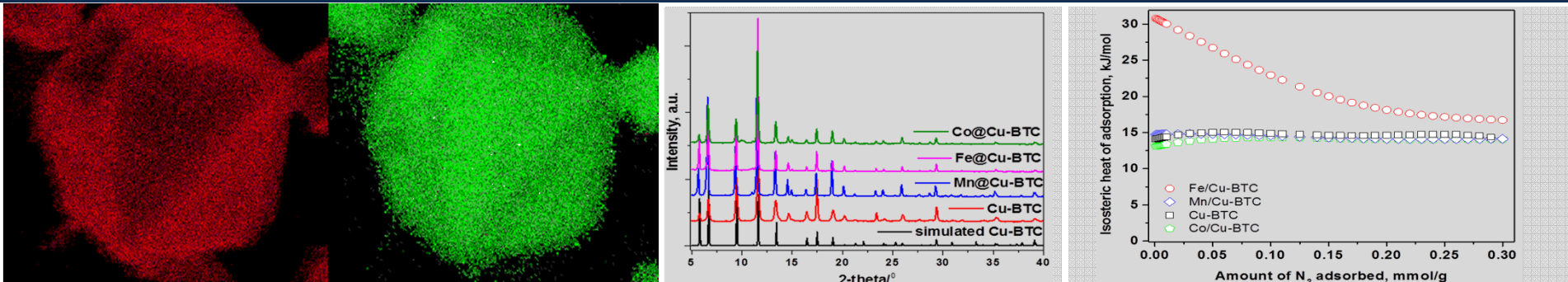


Exceptional service in the national interest



Oxygen Separations with MOFs via Predictive Modeling and Tuned Synthesis

Tina M. Nenoff, Dorina F. Sava Gallis, Marie V. Parkes, Jeffery A. Greathouse, Mark A. Rodriguez, Scott M. Paap, and Christopher R. Shaddix
 Sandia National Laboratories, Albuquerque NM & Livermore CA

November 13, 2014



This work is supported by the Laboratory Directed Research and Development Program at Sandia National Laboratories. Sandia National Laboratories is a multi-program laboratory managed and operated by Sandia Corporation, a wholly owned subsidiary of Lockheed Martin Corporation, for the U.S. Department of Energy's National Nuclear Security Administration under contract DE-AC04-94AL85000.

Outline

- I. Nenoff Research Portfolio
- II. Metal-organic Frameworks (MOFs) for Separations
- III. O₂ separations for Oxyfuel Combustion
 - a. Introduction
 - b. Modeling
 - c. Metal-substituted MOFs
 - d. SMOF-7
 - e. Oxyfuel, combustion and techno-economic analysis
- IV. Conclusions and Future Work

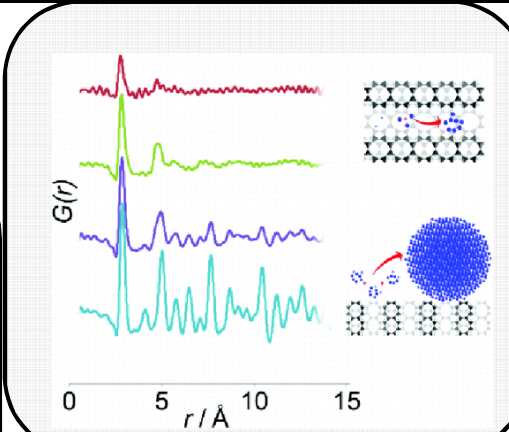
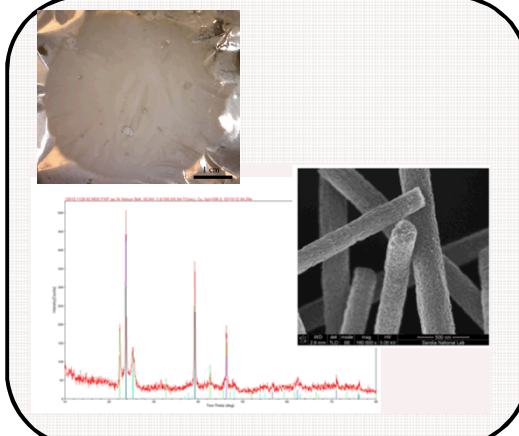
Outline

- I. Nenoff Research Portfolio
- II. Metal-organic Frameworks (MOFs) for Separations
- III. O₂ separations for Oxyfuel Combustion
 - a. Introduction
 - b. Modeling
 - c. Metal-substituted MOFs
 - d. SMOF-7
 - e. Oxyfuel, combustion and techno-economic analysis
- IV. Conclusions and Future Work

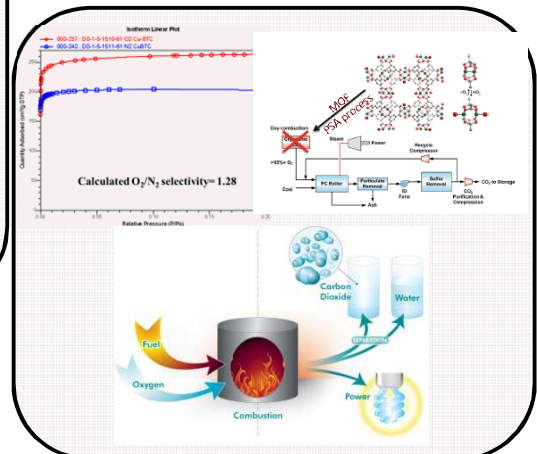
I. Nenoff Portfolio

Nanoparticle Occluded Zeolites: Catalysis and Separations

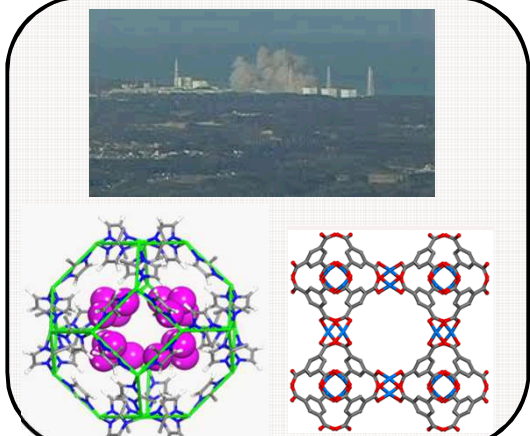
High Temperature Membranes for Gas Separations: Nanoporous Nanofibers



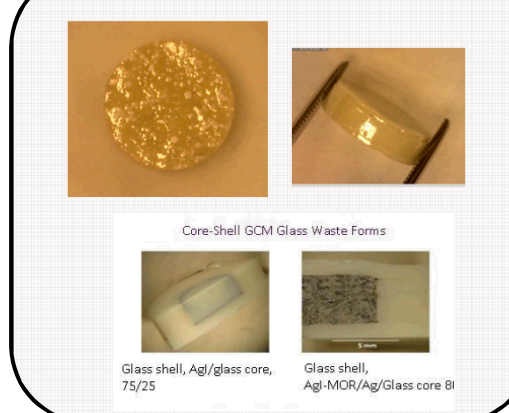
MOFs for Gas Separations & Use in Oxyfuel Combustion



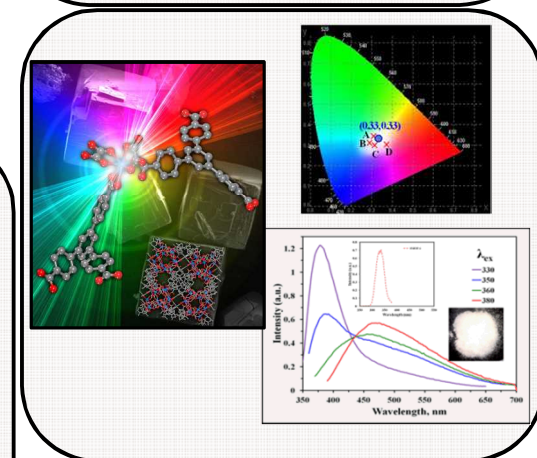
Materials design,
synthesis,
characterization,
and testing



Volatile Radionuclides Capture



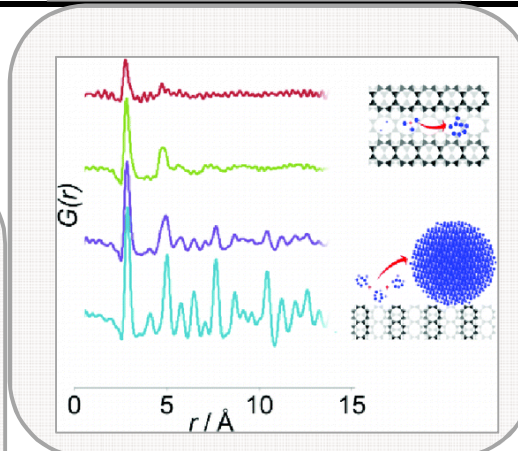
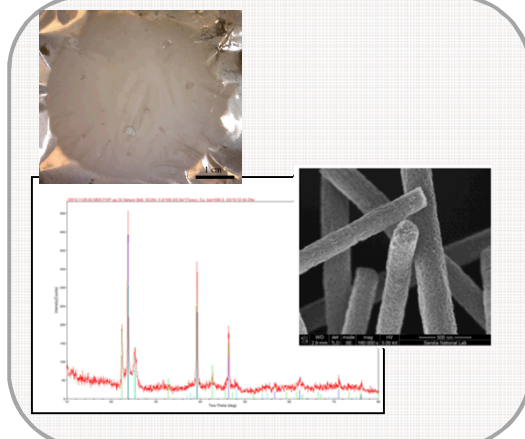
Nuclear Waste Glass & Ceramics



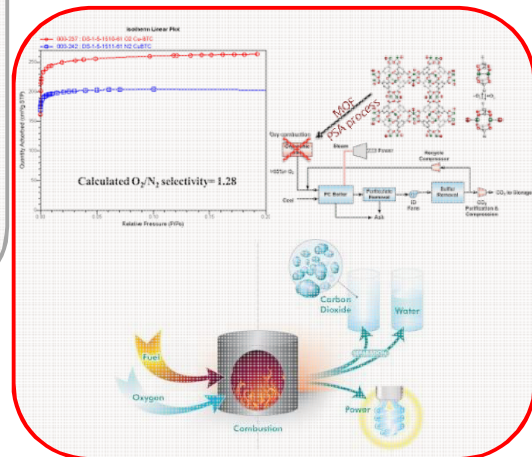
Solid-State Lighting

Nanoparticle Occluded Zeolites: Catalysis and Separations

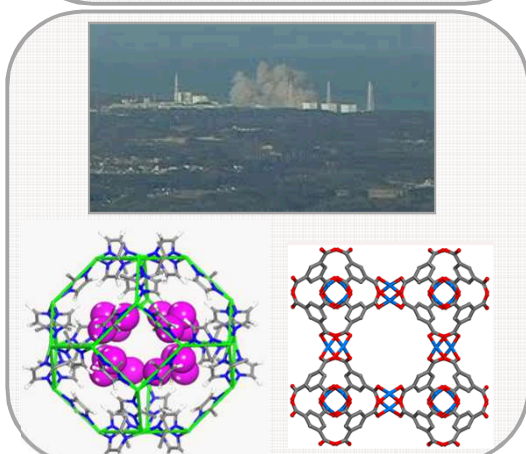
High Temperature Membranes for Gas Separations: Nanoporous Nanofibers



MOFs for Gas Separations & Use in Oxyfuel Combustion



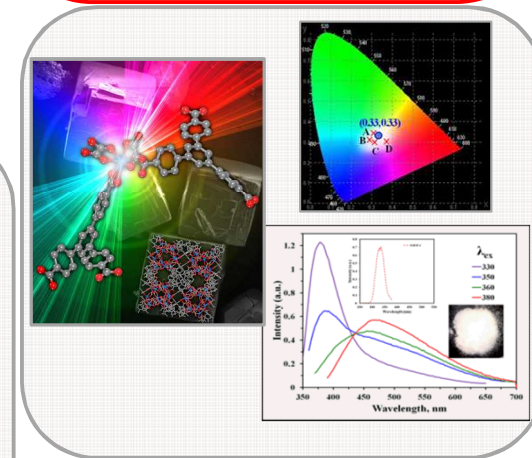
Materials design,
synthesis,
characterization,
and testing



Volatile Radionuclides Capture



Nuclear Waste Glass & Ceramics



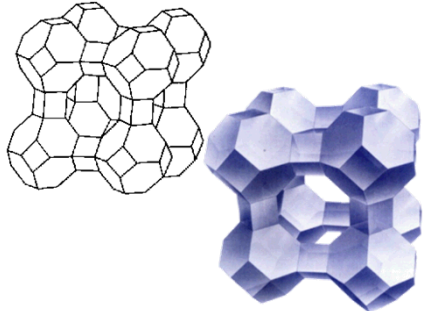
Solid-State Lighting

Outline

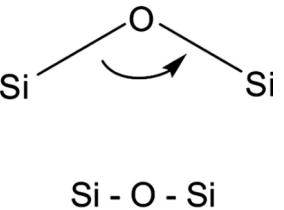
- I. Nenoff Research Portfolio
- II. Metal-organic Frameworks (MOFs) for Separations
- III. O₂ separations for Oxyfuel Combustion
 - a. Introduction
 - b. Modeling
 - c. Metal-substituted MOFs
 - d. SMOF-7
 - e. Oxyfuel, combustion and techno-economic analysis
- IV. Conclusions and Future Work

II. Metal-organic Frameworks (MOFs)

- **Zeolite Structures** are built from SiO_4 or $\text{Si}(\text{Al})\text{O}_4$ tetrahedra linked through bridging oxygen atoms;
 >150 structures, SA $\sim 100 \text{ m}^2/\text{g}$

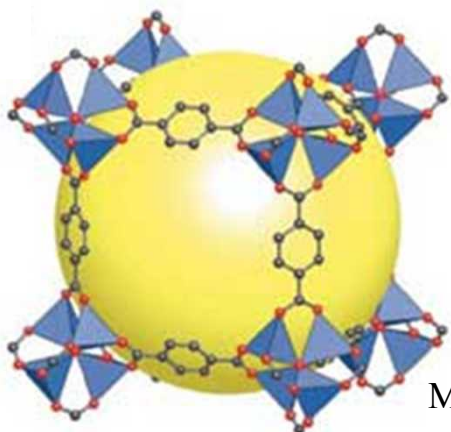


Zeolite 5A, opening $\sim 3.5\text{\AA}$
 $\text{Na}_{12}\text{Al}_{12}\text{Si}_{12}\text{O}_{48} \cdot 27\text{H}_2\text{O}$
commonly used in
PSA O_2 separations

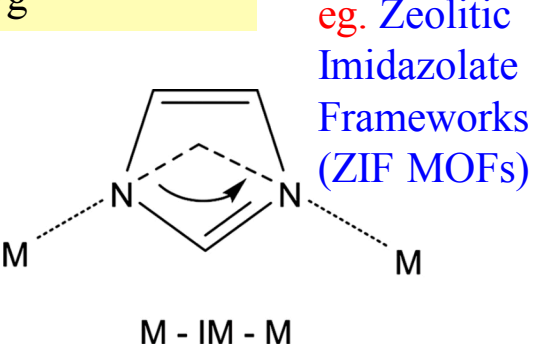


- Possible to build Metal-organic Frameworks (MOFs) with higher adsorption and selectivity by replacing zeolite linkers with **transition metals and organics**: Ultra high surface areas

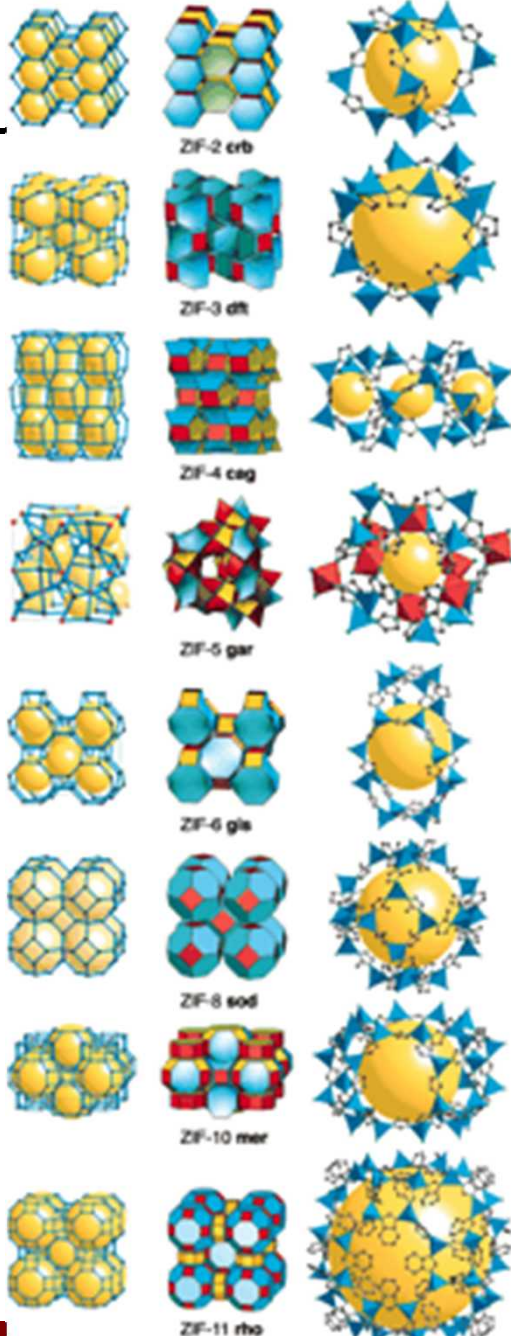
$>1000 \text{ m}^2/\text{g}$



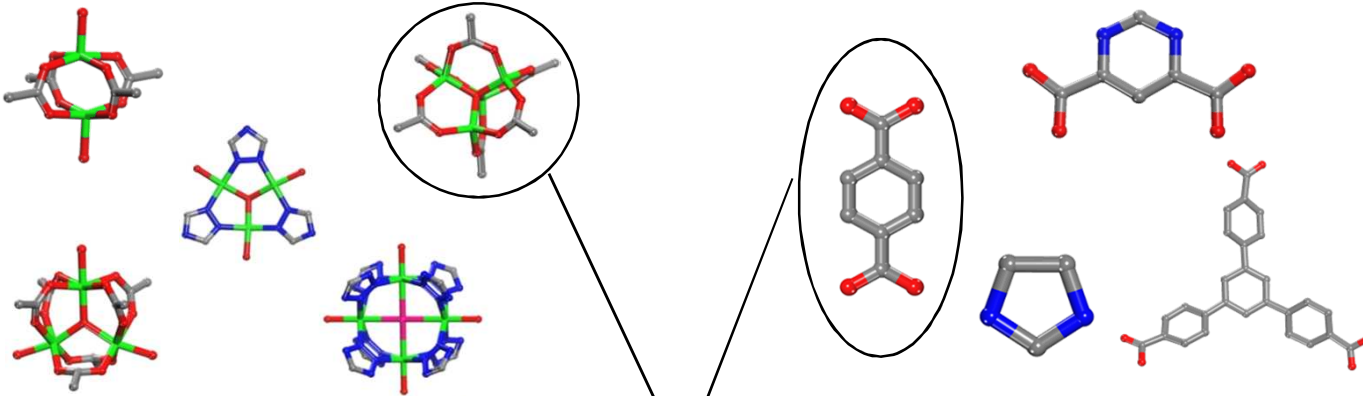
MOF-5: $\text{Zn}_4\text{O}(\text{BDC})_3$, opening 13.8\AA
 $\text{BDC}^{2-} = 1,4\text{-benzenedicarboxylate}$



eg. Zeolitic
Imidazolate
Frameworks
(ZIF MOFs)

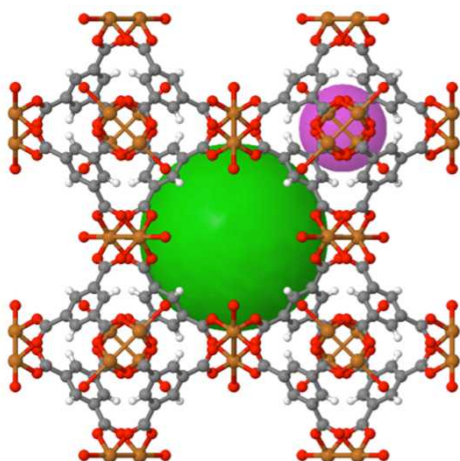


Metal-Organic Frameworks (MOFs)



Common metal clusters
(molecular building
blocks)

Organic Linking Units



HKUST-1 (Hong Kong University of Science and Technology), (Cu-BTC), is a metal organic framework (MOF) made up of copper nodes with 1,3,5-benzenetricarboxylic acid struts between them. The spheres represent the pore size within the framework which can be used for gas storage.

Mild Synthesis:¹
Cupric nitrate, H_2O
BTC, $EtOH/H_2O$,
Solutions mixed
 $110^\circ C$, 18 hrs
Xtals washed in $H_2O/EtOH$
Air dried

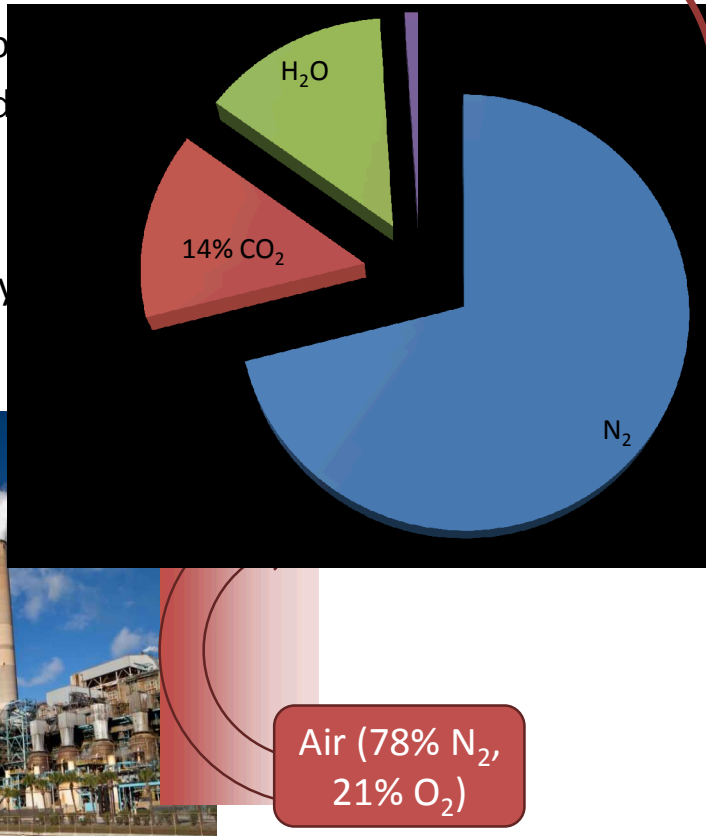
Outline

- I. Nenoff Research Portfolio
- II. Metal-organic Frameworks (MOFs) for Separations
- III. O₂ separations for Oxyfuel Combustion
 - a. Introduction
 - b. Modeling
 - c. Metal-substituted MOFs
 - d. SMOF-7
 - e. Oxyfuel, combustion and techno-economic analysis
- IV. Conclusions and Future Work

Oxyfuel for cleaner power plants

Benefits of using **oxyfuel** in power plants:

- Flue gas volume decreased
- Decreased NO_x emissions
- Greater thermal efficiency
- Increased energy efficiency
- Easier to capture CO₂



The generation of **oxygen-enriched air** is currently done by cryogenic distillation, an energy-intensive and expensive process.²

Potential Efficiency Improvement of MOFs Oxygen-from-Air-Separation Relative to State-of-the-Art

Cryogenic Air-Separation Unit (ASU) is state-of-the-art, but suffers from high power losses (primarily compression)

For example, for a 600 MW_e (gross) oxy-fuel power plant, 100 MW_e will be consumed by air-separation, resulting in an efficiency decrease of 10 percentage points ¹⁻²

Similarly, for application to a glass melting furnace, Schepp³ estimates oxygen production accounts for $\approx 10\%$ of energy use

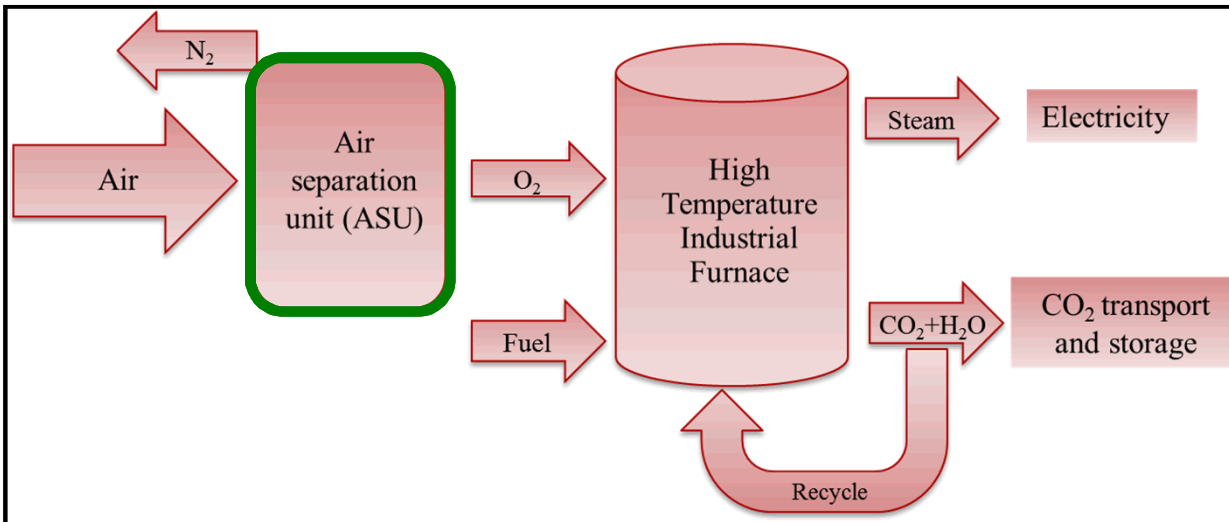
MOFs-based air separation, with its minor power requirements for pressurization, is anticipated to ensure major energy and cost savings

target: 25% savings



Air Liquide cryogenic ASU at Callide 30 MW_e Oxy-Fuel Power Plant Demonstration

O₂/N₂ air separations with MOFs to Increase the Efficiency of the *ASU*



Process Development:

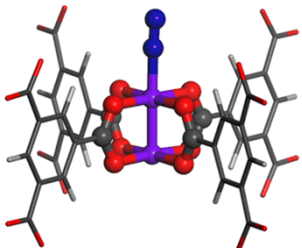
MOFs to replace zeolites in PSA
Processes for the energy efficient production of pure O₂ from air at temperatures up to ambient.

- Oxygen-enriched (oxy-fuel) combustion: burning the fossil fuel in an O₂ rich atmosphere resulting in high efficiency burning, easily captured CO₂, little/no NO_x production
- Purification of O₂ limiting step:
 - (1) Cryogenic, costly & energy intensive process (primarily compression) for high purity O₂ (99.9%),
 - (2) Pressure Swing Adsorption (PSA), use of zeolites for less costly separation but lower purity O₂ (94%)
- Replace Zeolites in PSA with **high surface area, high capacity and high selectivity Metal-organic Framework (MOFs)** for O₂ separation from air

Integrated Research Plan: Modeling, Materials Development, Combustion Testing, & Systems Analysis

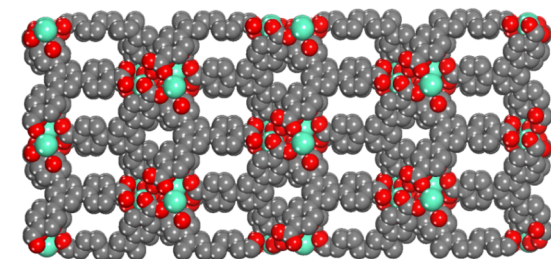
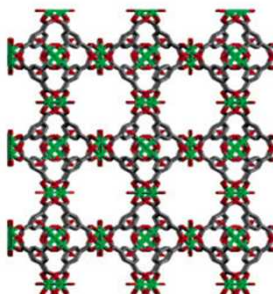
Predictive molecular modeling

Predictive molecular modeling designed to *measure the binding energy for O₂ and N₂* on coordinatively unsaturated metal sites in MOFs



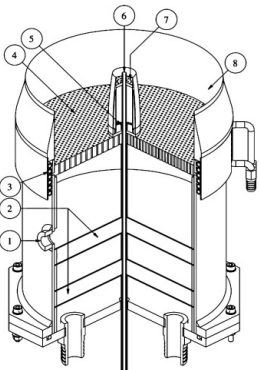
Materials development

Guided by the modeling results, experiments are directed at both the *synthesis of analogs of known/modified materials and of novel frameworks*.



New burner design

New lab burner constructed to mimic practical oxy-fuel combustion in industrial applications: coupling burner design and oxy-fuel combustion to radiant heat transfer



Burner number	Description
1	Flashback over-pressure sensing port
2	Glass head filled cavities
3	Cooling water coil
4	Coolant preheated baseplate
5	Flame measurement slot
6	Central jet exit
7	Pilot perforated baseplate
8	Cowflow collar

Schematic diagram of the modified version of the Cabra Burner developed by Dunn et al. (Combust. Flame, 2007, 151, 46)- studying flame attachment in hot combustion products

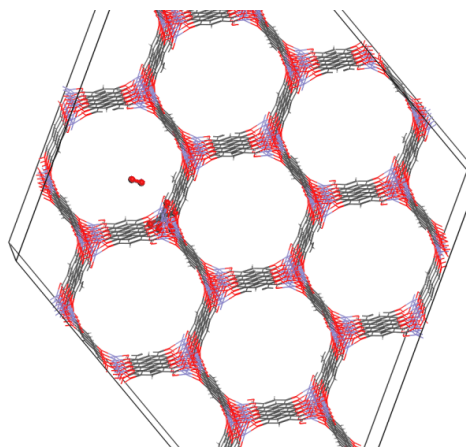
Techno-Economic Modeling

Data input to Systems Analysis for calculations of efficiency improvements of combined developed MOFs into Oxy-fuel Process Stream

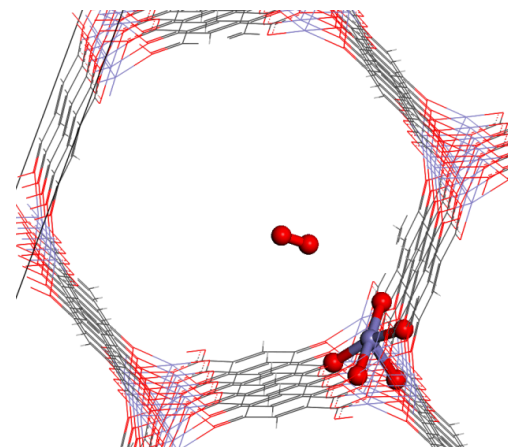
Input information/data from combustion to systems analysis for calculation of percent efficiency improvements

III b. Modeling: DFT Simulations

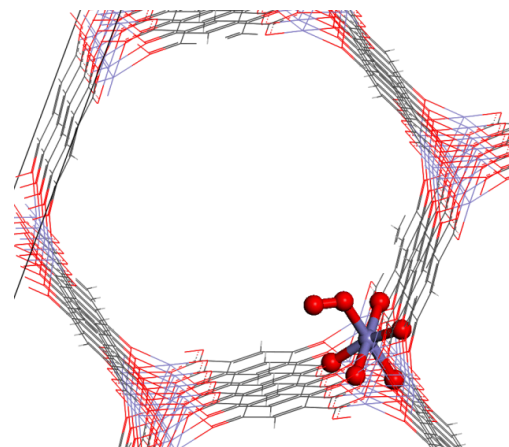
- ***Molecular-level Details of Metal-O₂ and Metal-N₂ Binding Energies and Geometries***
- MOFs with coordinatively unsaturated metal centers are promising materials for O₂/N₂ separations
- Two prototypical MOFs from this category, Cr₂(BTC)₃¹ (**HKUST-1**) and Fe₂(DOBDC)² (**MOF-74**)
- both show preferential adsorption of O₂ over N₂
- Plane wave DFT calculations were performed on periodic structures in the Vienna Ab initio Simulation Package (VASP)
- Binding geometries for side-on and bent O₂ and bent and linear geometries for N₂ were evaluated
- Static binding energies for O₂ and N₂ at 0 K



MOF with O₂ in pore

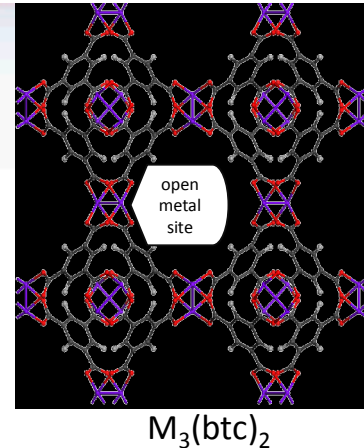
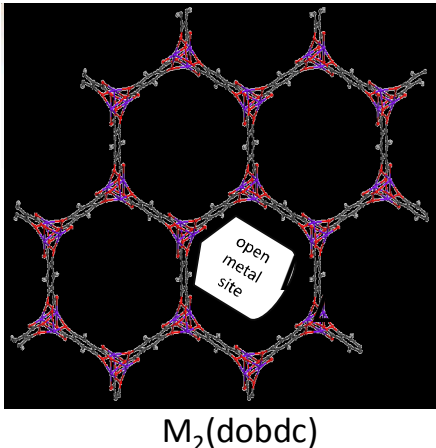


O₂ ready to bind to metal



O₂ bound to metal

DFT modeling of Oxygen Adsorption in Varied Metal-Centered MOFs



MOF metal sites = separate O_2/N_2 by differences in bonding & electronic properties

Plan wave density functional theory (DFT) calculations were performed on periodic structures of each MOF in the Vienna ab initio simulation package (VASP) with the Perdew-Burke-Ernzerhof (PBE) functional including dispersion corrections (DFT-D2). Geometries were optimized and static binding energies ($\Delta E_{\text{O}_2}, \Delta E_{\text{N}_2}$) were calculated by

$$\Delta E_{\text{O}_2} = E_{\text{MOF+O}_2} - E_{\text{MOF}} - E_{\text{O}_2}$$

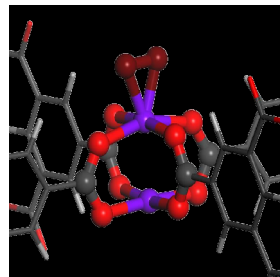
The differences in binding energies ($\Delta\Delta E$) for oxygen and nitrogen were calculated by

$$\Delta\Delta E = -(\Delta E_{\text{O}_2} - \Delta E_{\text{N}_2})$$

Attention Paid to Bonding Geometries

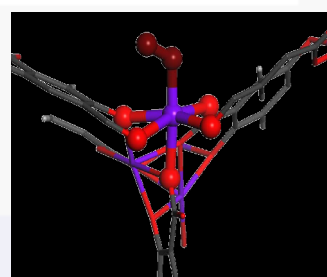
Side-on bonding

$\Delta M\text{-X-X} 67^\circ - 71^\circ$



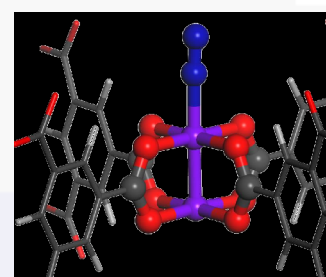
Bent bonding

$\Delta M\text{-X-X} 116^\circ - 159^\circ$



Linear bonding

$\Delta M\text{-X-X} 165^\circ - 179^\circ$



Sandia Red Sky Super Computer: Transition Metal-MOF-O₂ or N₂ Screening

Bonding geometry as a function of metal

Bonding geometries of O ₂ binding to M ₃ (btc) ₂			
Metal (M)	Binding Energy (kJ/mol)	M-O Distance (Å)	Bonding Mode*
Sc	-402	1.91	Side-on
Ti	-331	1.85	Side-on
V	-165	1.83	Side-on
Cr	-107	1.98	Side-on
Mn	-66	1.87	Bent
Fe	-70	1.97	Bent
Co	-68	1.93	Bent
Ni	-87	1.95	Bent
Cu	-116	2.32	Bent
Zn	-25	2.27	Bent

Bonding geometries of O ₂ binding to M ₂ (dobdc)			
Metal (M)	Binding Energy (kJ/mol)	M-O Distance (Å)	Bonding Mode*
Sc	-214	1.93	Side-on
Ti	-350	1.83	Side-on
V	-279	1.86	Side-on
Cr	-150	1.83	Side-on
Mn	-107	1.88	Bent
Fe	7	2.04	Bent
Co	-82	1.84	Bent
Ni	-48	1.95	Bent
Cu	-23	2.35	Bent
Zn	-25	2.28	Bent

Bonding geometries of N ₂ binding to M ₃ (btc) ₂			
Metal (M)	Binding Energy (kJ/mol)	M-N Distance (Å) [†]	Bonding Mode*
Sc	-47	2.24	Bent
Ti	-27	2.36	Bent
V	-21	2.28	Linear
Cr	-36	2.73 (nb)	Bent
Mn	52	2.32	Linear
Fe	-8	1.96	Linear
Co	-57	1.95	Linear
Ni	-76	1.99	Linear
Cu	-105	2.34	Bent
Zn	-39	2.22	Linear

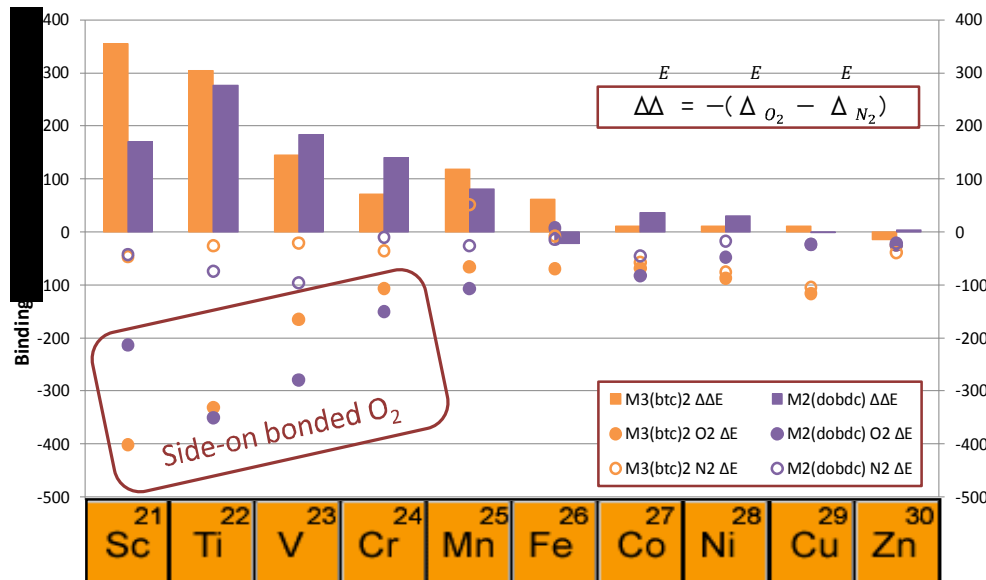
Bonding geometries of N ₂ binding to M ₂ (dobdc)			
Metal (M)	Binding Energy (kJ/mol)	M-N Distance (Å) [†]	Bonding Mode*
Sc	-43	2.36	Linear
Ti	-74	2.07	Linear
V	-96	1.98	Linear
Cr	-10	1.88	Linear
Mn	-26	2.37	Bent
Fe	-14	3.58 (nb)	Bent
Co	-46	1.93	Linear
Ni	-17	2.92 (nb)	Bent
Cu	-24	2.92 (nb)	Bent
Zn	-22	2.64 (nb)	Linear

* Side-on bonding mode corresponds to M-X-X angle 67°-71°; Bent bonding mode corresponds to M-X-X angle 94°-159°; Linear bonding mode corresponds to M-X-X angle 165°-179°.

[†] (nb) indicates that the M-X interatomic distance is too long to represent a bonding interaction.

Transition to Quantum Calculations to Estimate Metal-Oxygen Binding Energy

Binding Energy Calculated as a Function of Metal Site

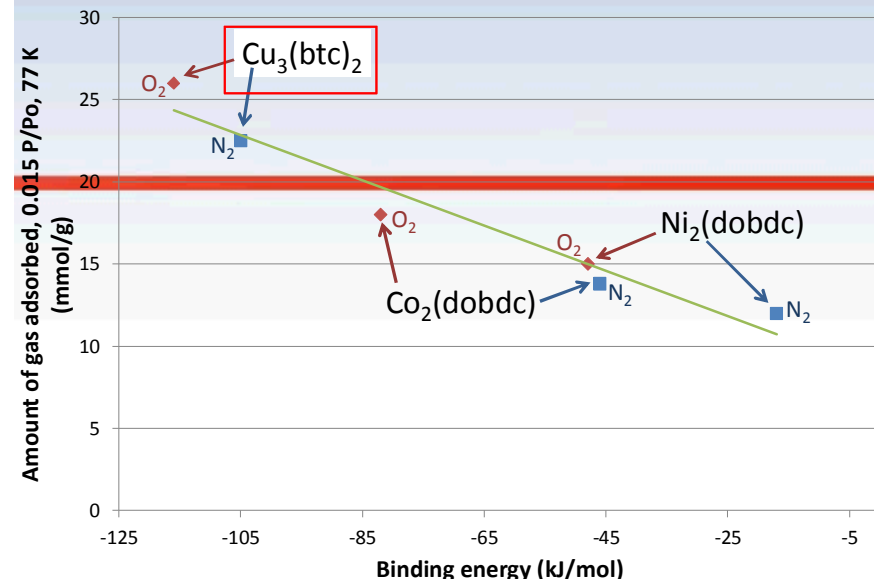


Parkes, M.; Sava Gallis, D. F.; Greathouse, J.A.; Nenoff, T.M.
"Screening MOFs for O₂/N₂ Separations: Role of MOF Metal Center",
2014, in preparation.

Marie Parkes, Sanibel Conference, Top Prize - Poster, 2014

Experimental Confirmation

Low-temperature, low-pressure O₂ and N₂ adsorption measurements were done for three MOFs: Cu₃(btc)₂, Co₂(dobdc), and Ni₂(dobdc).



Excellent correlation between simulated binding energies and low-temperature, low-pressure experimental gas uptake.

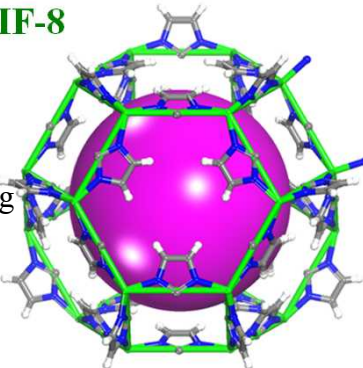
MOFs Platforms Used for O₂/N₂ Sorption Studies: Known/Literature and Sandia

O₂: 3.46 Å ; N₂: 3.64 Å

Al-MIL-53

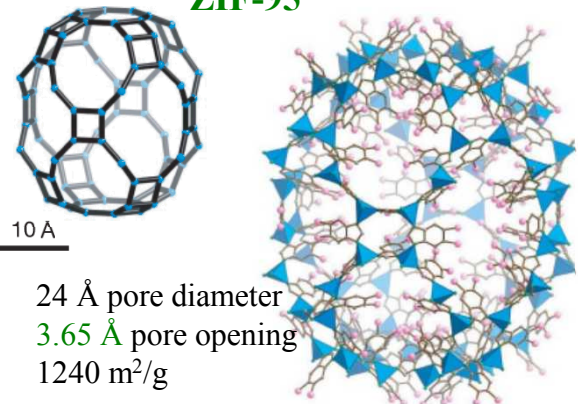
ZIF's successful on single gas
Syngas separations: *Size Selectivity*

ZIF-8



11.6 x 14.6 Å pore diameter
3.4 Å pore opening
1100 m²/g

ZIF-95

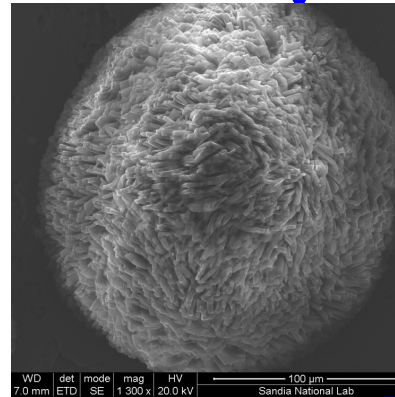
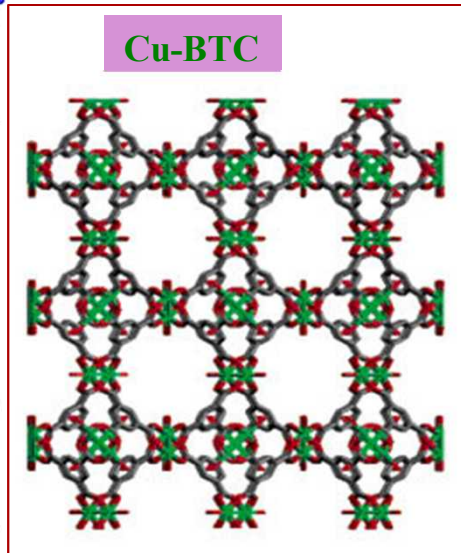


Open Metal Centers

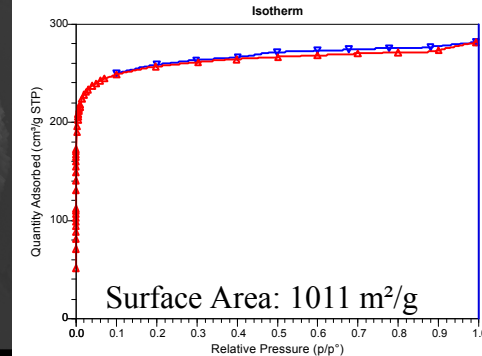
Fe-HKUST

Fe-BTC

Cu-BTC

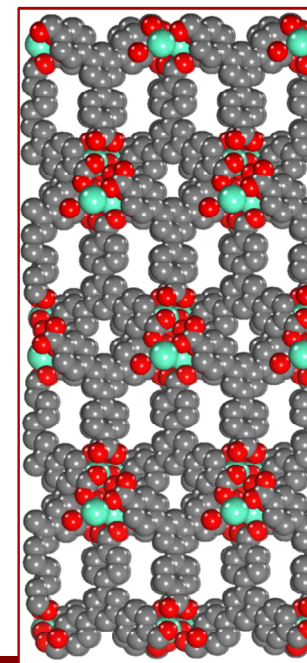


SMOF-3



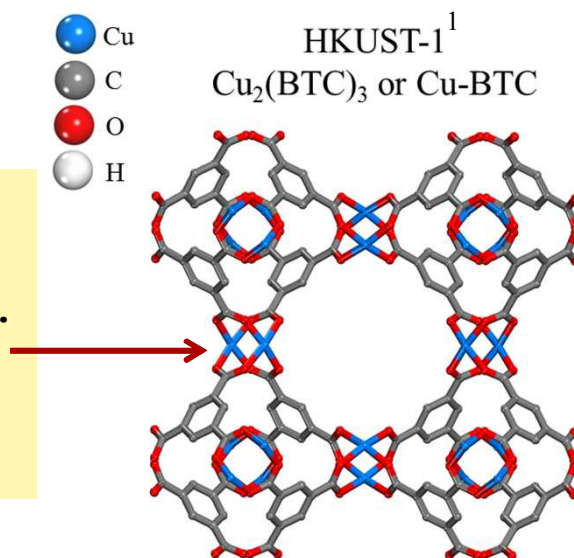
Type I isotherm, steep rise indicates strong adsorbent-adsorbate interactions

SMOF-7



III c. Metal Substituted MOFs: Targeted Synthesis of Porous Mn-, Fe- and Co- Cu-BTC

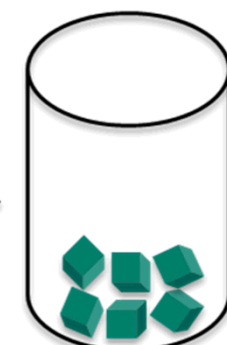
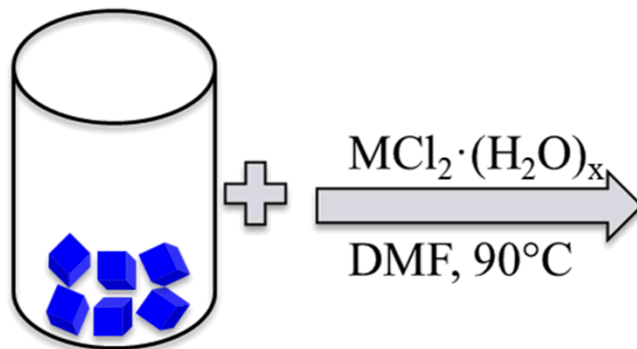
MOF metal centers can be considered as **Site isolated molecular units**. Mild reaction **ion exchange** without detriment to the entire MOF framework unit



MOF metal Substitution with Retention of Porosity: 2 approaches

1. M-substituted Cu-BTC: Cr, Mo, Ru, Ni (Ru & Ni much lower than expected surface area of $\sim 1100 \text{ m}^2/\text{g}$)
2. Porphyrin-templated Mn-, Fe- & Co-Cu-BTC analogues² known, *no measurable accessible porosity*

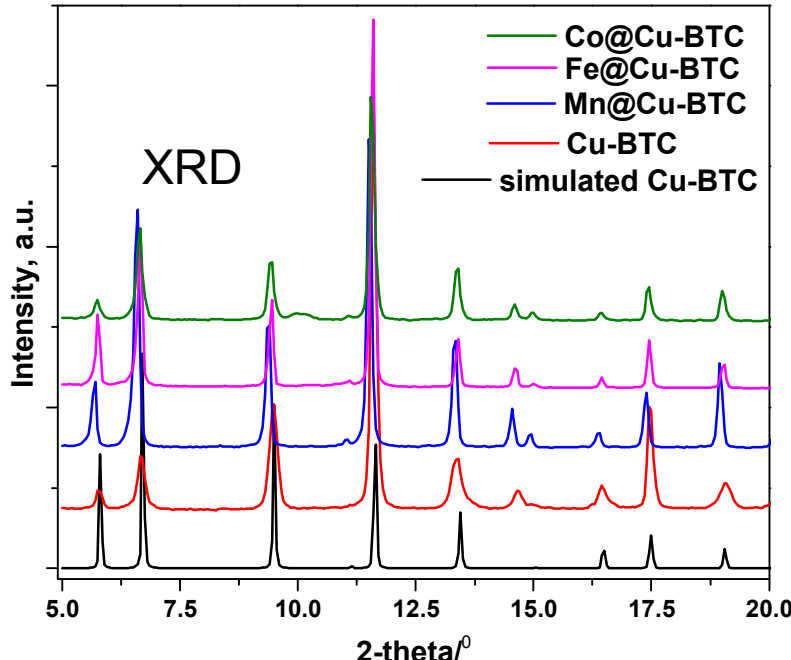
Postsynthetic metal ion exchange³



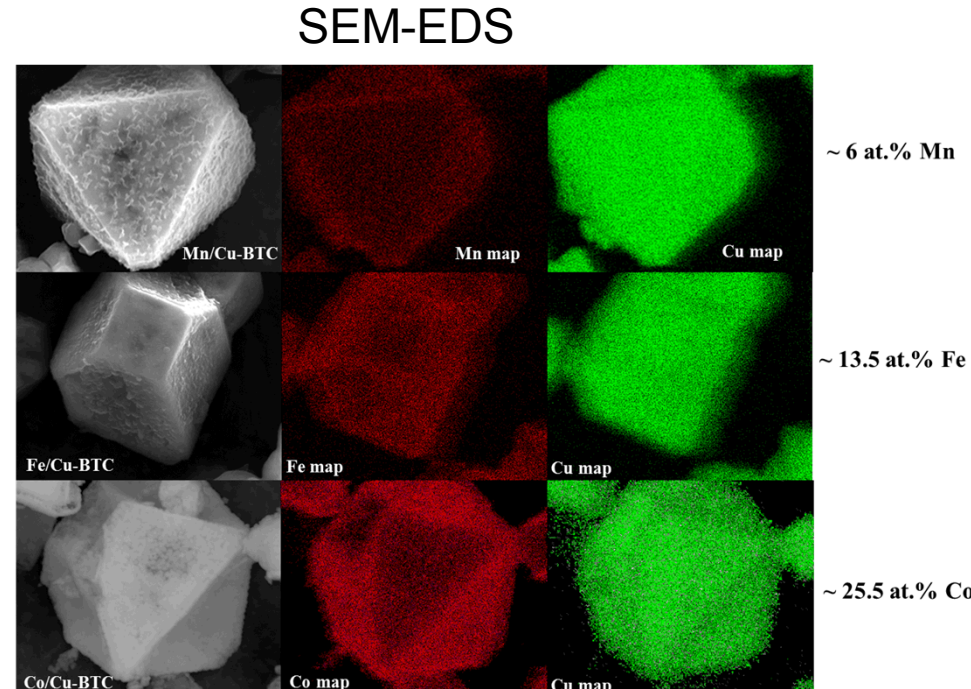
$M = \text{Mn, Fe, Co}$

Sava Gallis, D. F.; Parkes, M.; Greathouse, J.A.; Nenoff, T.M. "O₂/N₂ separations with Metal substituted MOFs", 2014, submitted, *Chem. Mater.*

Confirmation of In-Framework Metal Substitution – Unit Cell Expansion & Elemental Mapping



	Expansion (\AA)	M-O average bond length (\AA)
Cu-BTC	–	1.7
Co/Cu-BTC	0.043	2.08
Fe/Cu-BTC	0.019	2.0
Mn/Cu-BTC	0.030	2.17

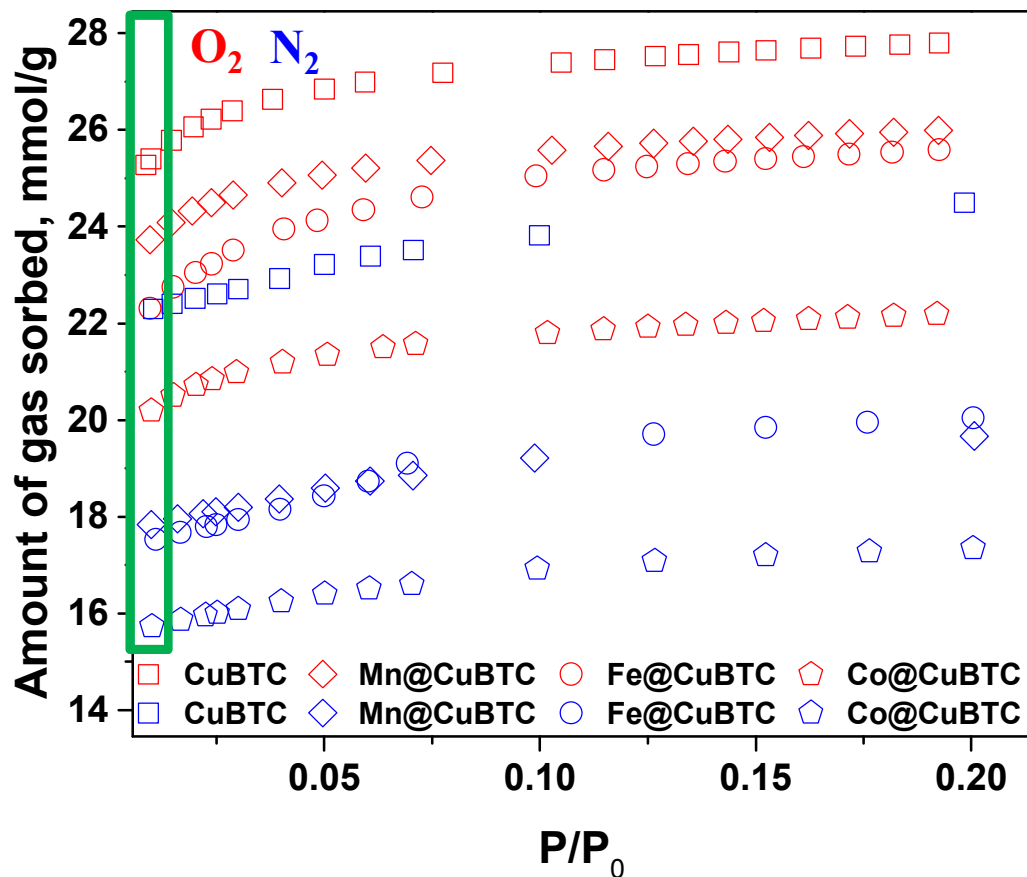


Excellent DFT and Experiment Correlation at Low Temperature and Low Pressure

Cu>Mn>Fe>Co (DFT)
Cu>Mn>Fe>Co (exp)

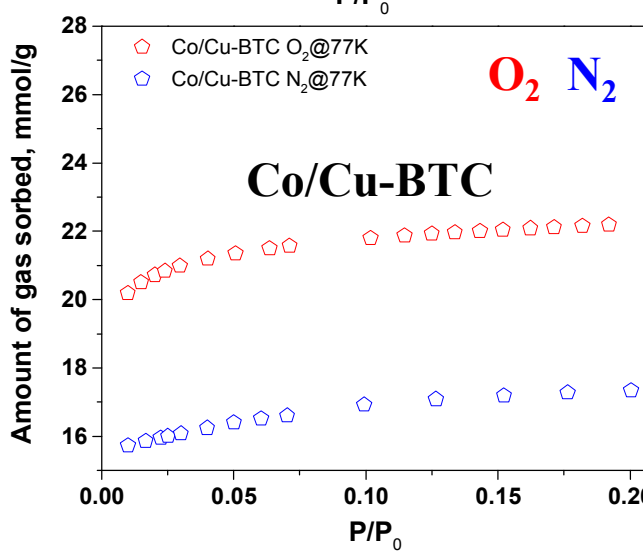
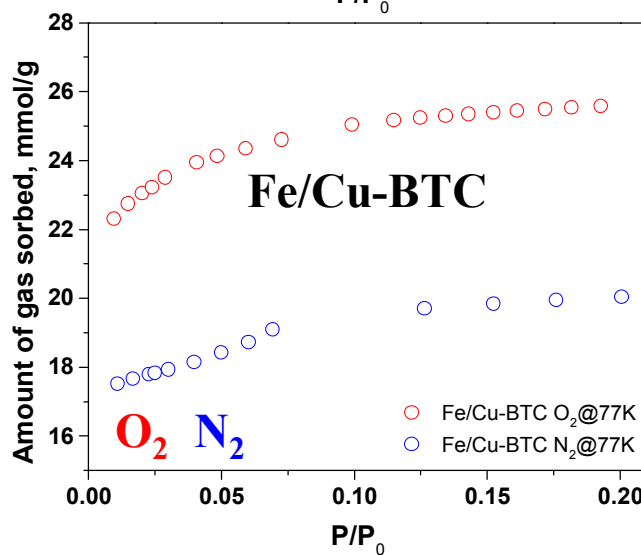
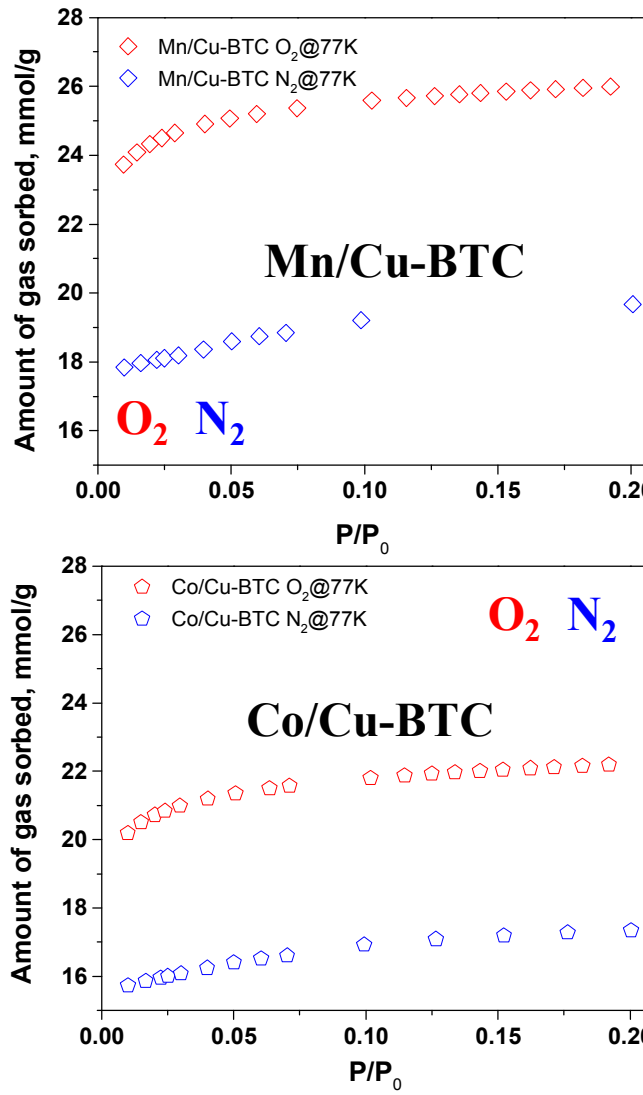
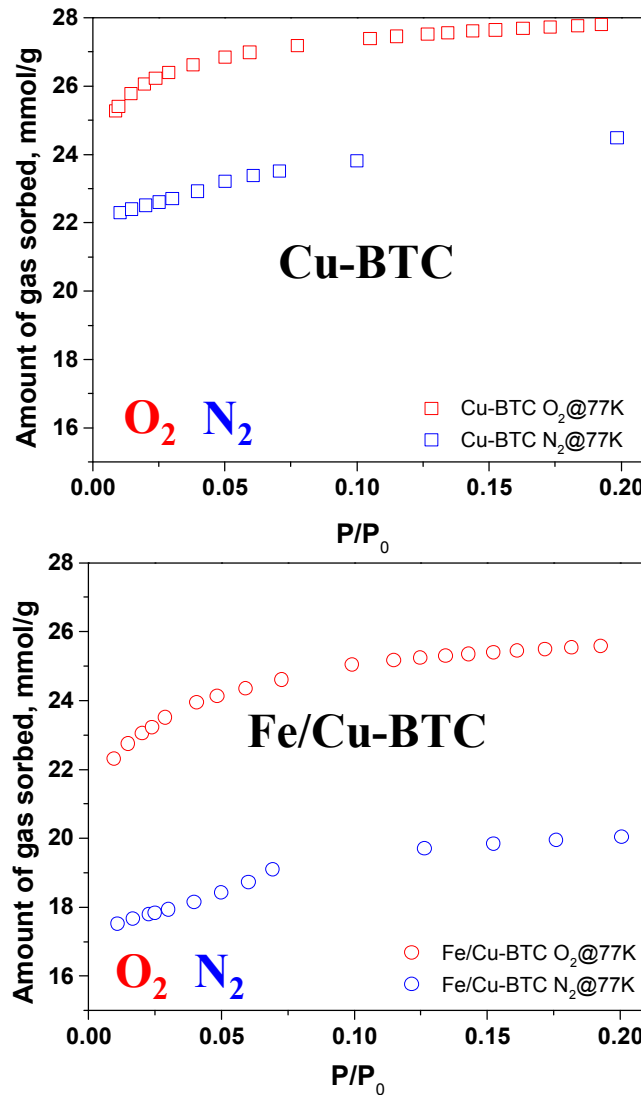
	DFT O ₂ binding energy, kJ/mol	DFT N ₂ binding energy, kJ/mol
Cu-BTC	-116	-105
Mn/Cu-BTC	-113	-97
Fe/Cu-BTC	-110	-92
Co/Cu-BTC	-104	-93

For uptake at the lowest partial pressure measured ($\sim 0.01 P/P_0$)



O₂ (red) and N₂ (blue) adsorption isotherms measured at 77K on pristine Cu-BTC and Mn-, Fe-, and Co-substituted samples

77 K: All Samples have *Higher* O₂ Loadings over N₂

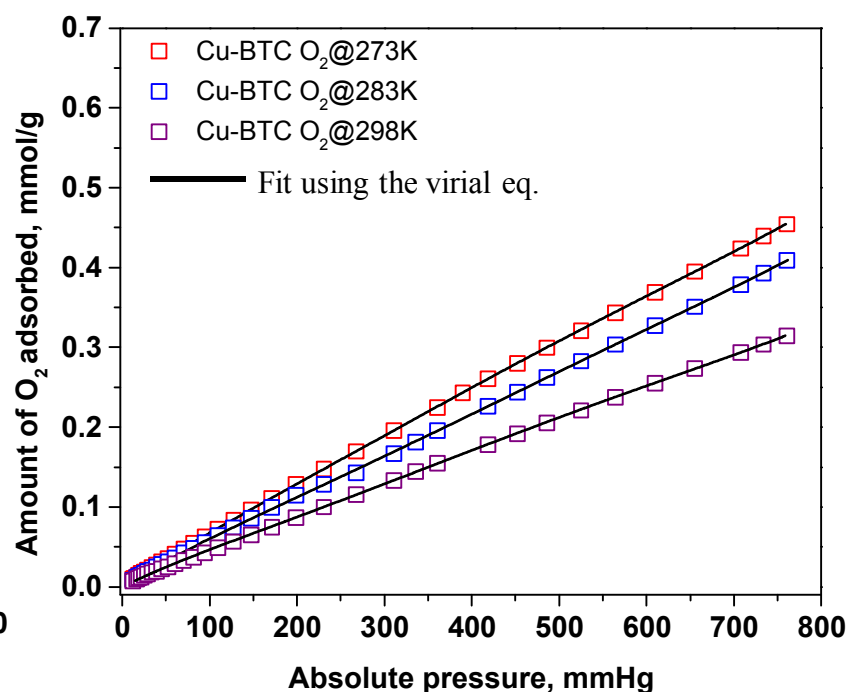
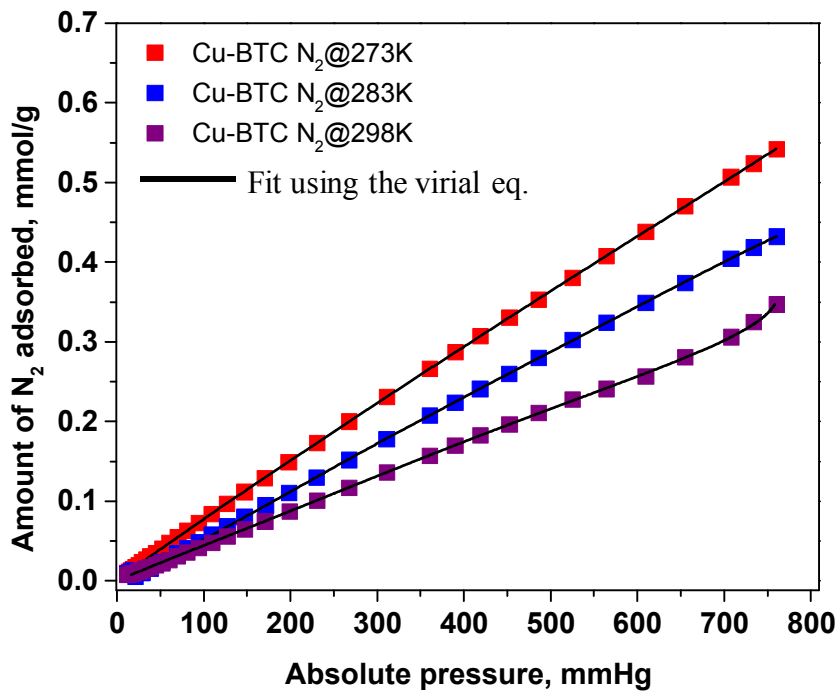


The highest O₂/N₂ selectivity is observed for the Mn/Cu-BTC sample

273-298 K: As Temperature Increases, O₂ Loadings Decrease Relative to N₂

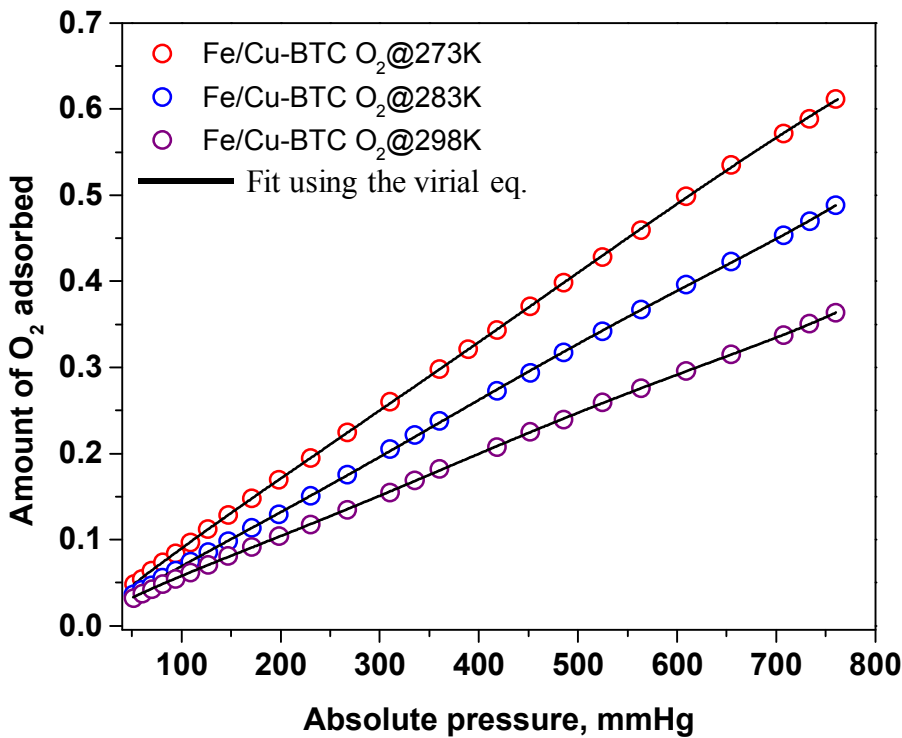
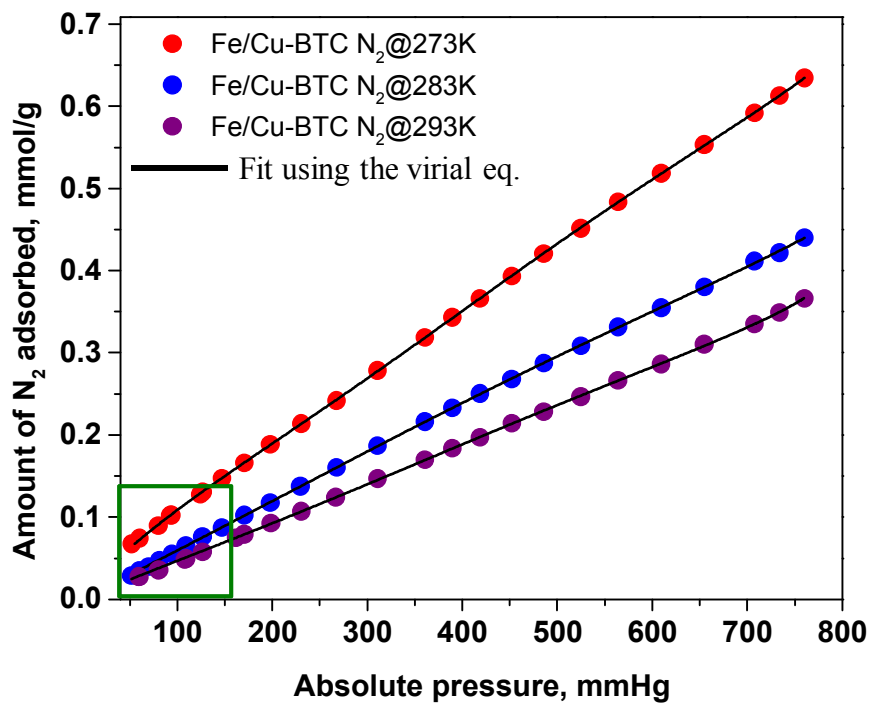
Isotherms in the 273-298K range, *independently* fitted using a modified virial equation:

$$\ln P = \ln N + \frac{1}{T} \sum_{i=0}^m a_i N^i$$



Similar behavior noted for the Mn- and Co/Cu-BTC samples

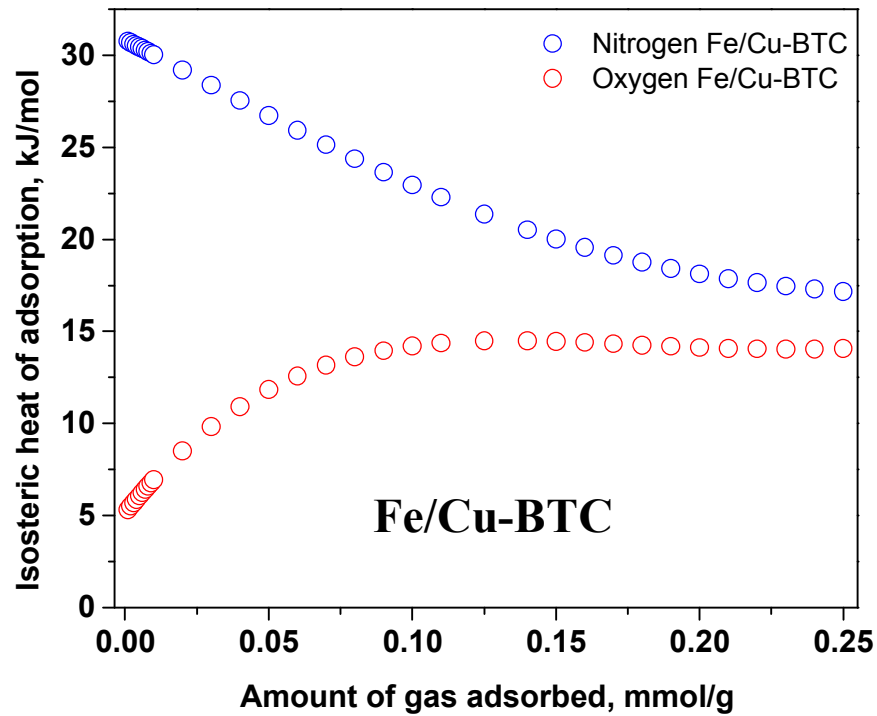
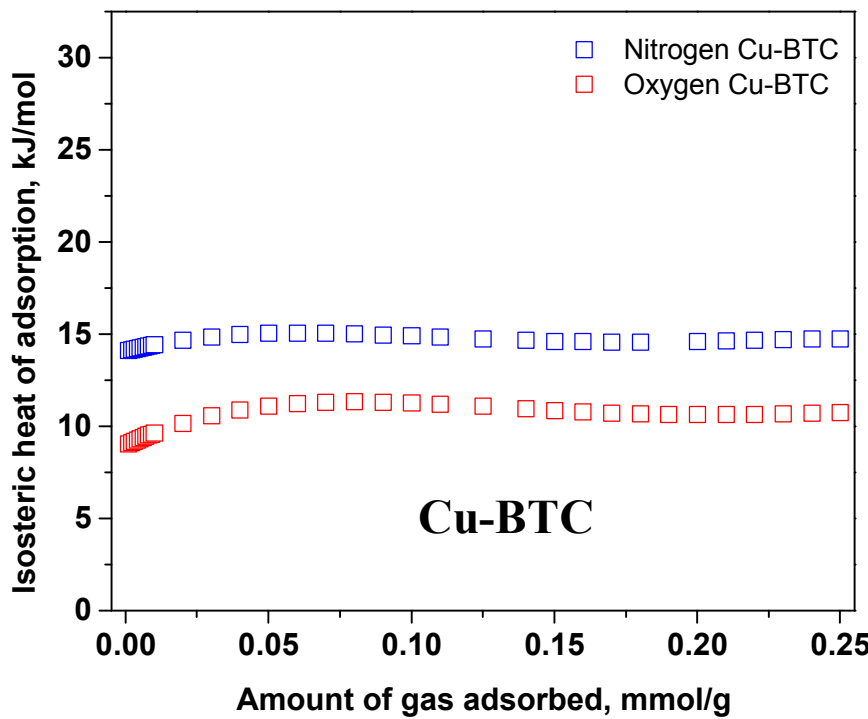
N_2 @273 K in Fe/Cu-BTC Trend Deviation: Slightly Higher N_2 Uptake at Lowest Loading Levels (at lowest pressures)



N_2 and O_2 adsorption isotherms measured at 273, 283, and 298K on Fe/Cu-BTC

Similar N_2 and O_2 uptake for Fe/Cu-BTC in the room temperature range

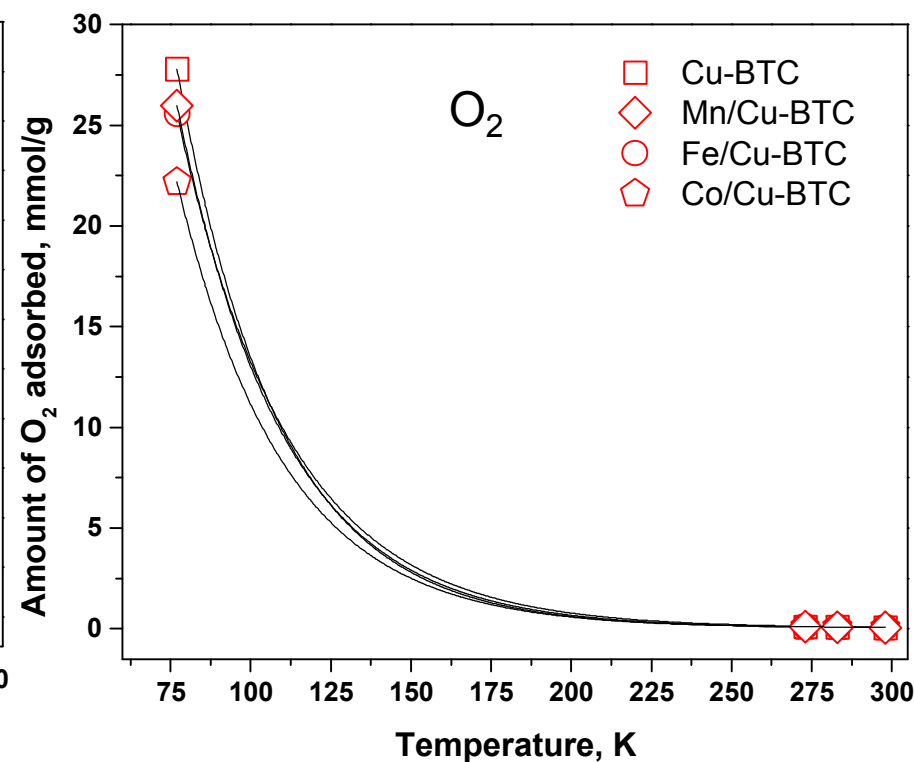
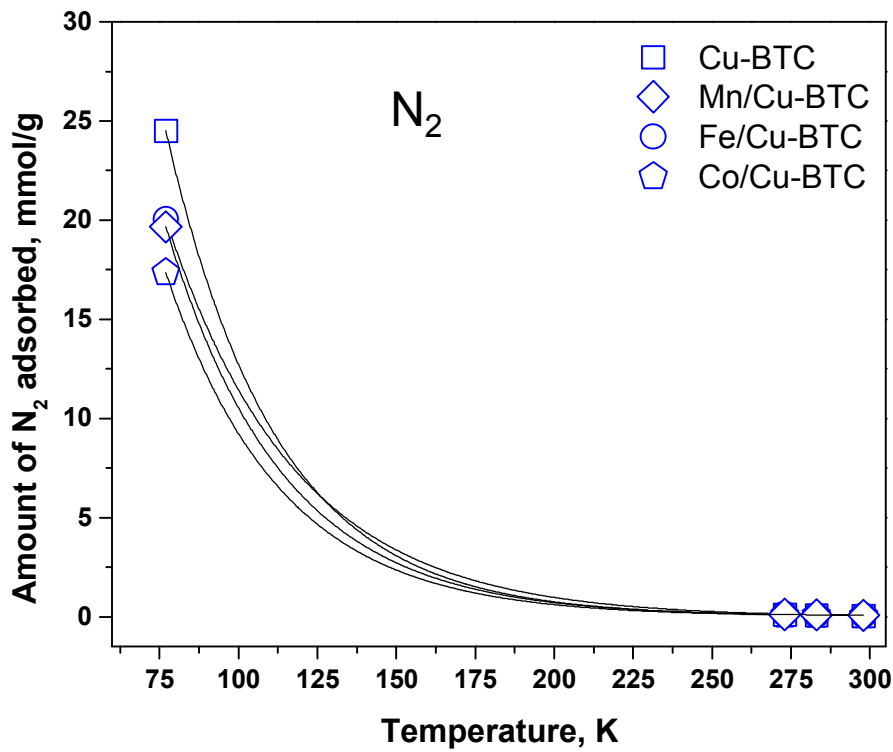
Isosteric Heats of Adsorption for O₂ (red) and N₂ (blue) Comparison of Cu-BTC vs Fe/Cu-BTC Data



The 0 K DFT *binding energy* calculations **do not correlate** as well with experimental data from **273-298 K**

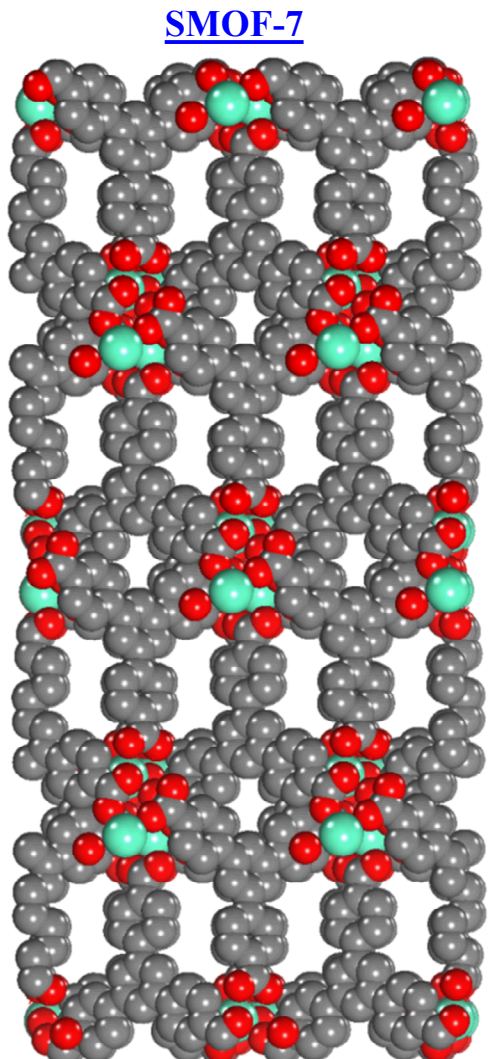
At 77K, Metal Sites Play an Important Role, while at 273 - 298 K Metal Sites have a *Smaller Effect*

The temperature dependency of the N_2 and O_2 uptake at ~ 0.2 atm and 77, 273, 283, and 298 K

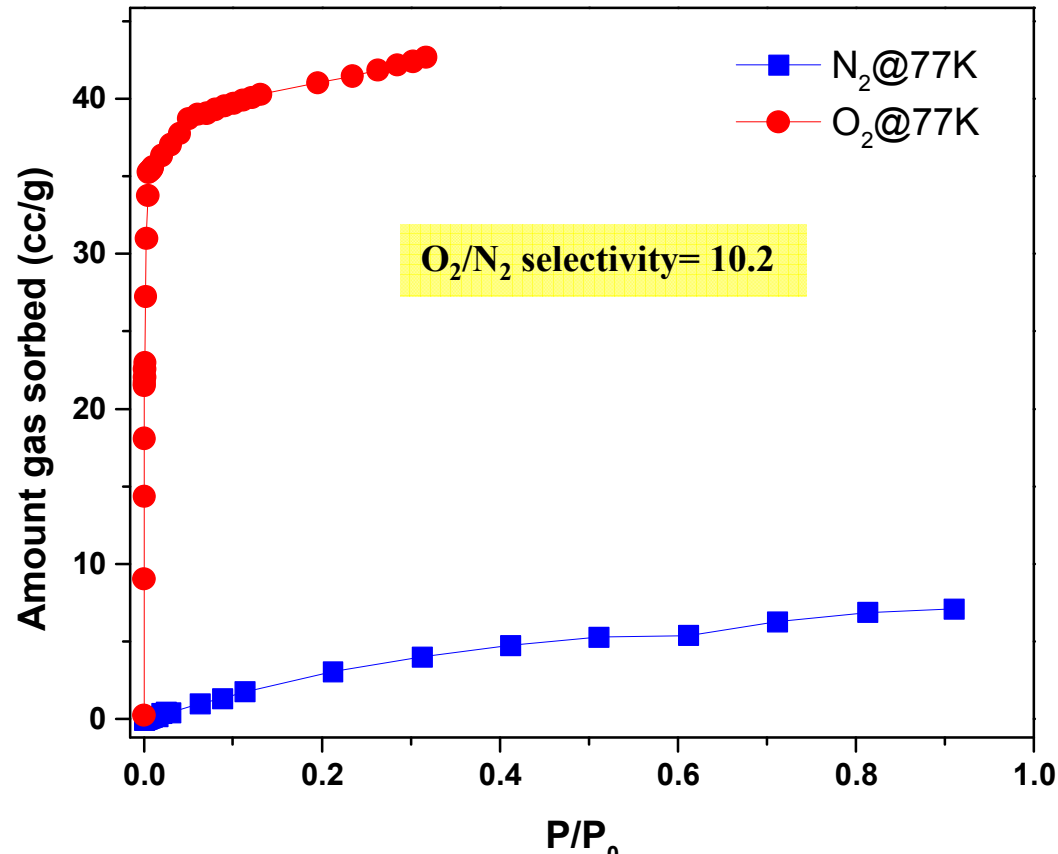


Distinct transition point temperature where the metal sites dependence on the O_2 and N_2 uptake is inverted

III d: SMOF-7, High Selectivity, Low Capacity for O₂



D. Sava Gallis, T. M. Nenoff,
US Patent Pending, 2014



O₂ vs. N₂ Single Gas Sorption Isotherm, at 77K

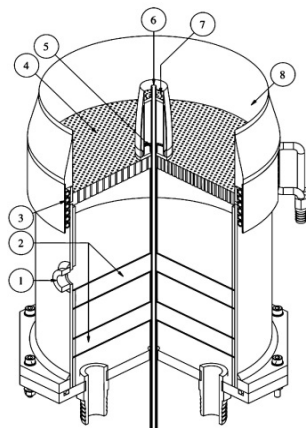
7 x 4.4 Å pore diameter, 5.1 Å pore opening, 7-17 m²/g

Combine Experiment MOFs Gas Separations Data into Flame / Combustion Testing

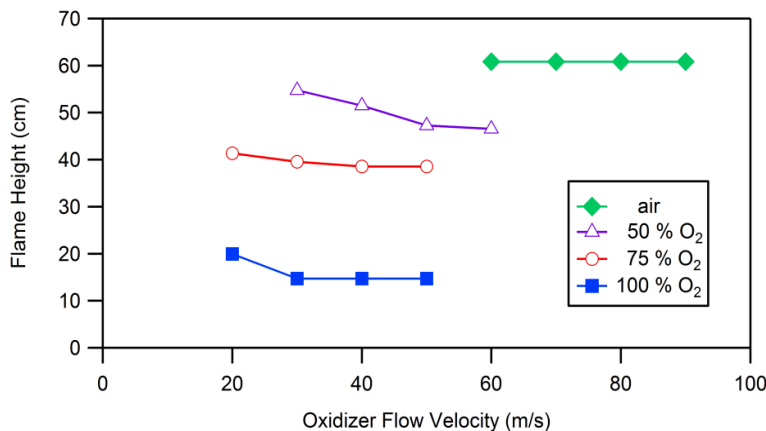
Enhanced O₂/N₂ via MOF -> heat/radiation improvement w/oxyfuel -> improved efficiency

- 1) Study of non-premixed oxygen-enriched and oxy-fuel flames using a non-premixed turbulent jet flame burner
- 2) Measurement of radiant flux for accurate determination of flame radiation
- 3) Measurement of soot concentration in flames planar laser-induced incandescence measurements (LII)
- 4) Allow for the calculation of the contribution of the soot to total radiant heat transfer of the flames
- 5) **Data input to Systems Analysis for calculations of efficiency improvements of combined developed MOFs into Oxyfuel Process Stream**

Coupling of Burner design and Oxy-fuel Combustion to Radiant Heat Transfer



Balloon number	Description
1	Flameback over-pressure sensing port
2	Glass bell jar filled cavities
3	Cooling water coil
4	Co-flow perforated baseplate
5	Pilot mixture feed exit
6	Central jet exit
7	Pilot perforated baseplate
8	Co-flow collar



Initial calculated/predicted flame heights when using a 1/8", 0.020 wall stainless steel tube to deliver methane to the Dunn burner.

The volumetric flow of methane is always equal to $\frac{1}{2}$ the flow of oxygen, to maintain stoichiometric combustion conditions.

Preliminary Investigation of Oxygen-Enriched NG Flames

Performed preliminary testing performed with oxidizers of pure oxygen and with 50% O₂ in N₂, using an overall equivalence ratio of 1, with a constant methane flow

- Velocity (Re) of oxidizer flow is 50% lower when using pure O₂, making for taller flame (slower mixing)
- Soot formation is enhanced when using pure O₂ (higher temperatures, slower mixing)



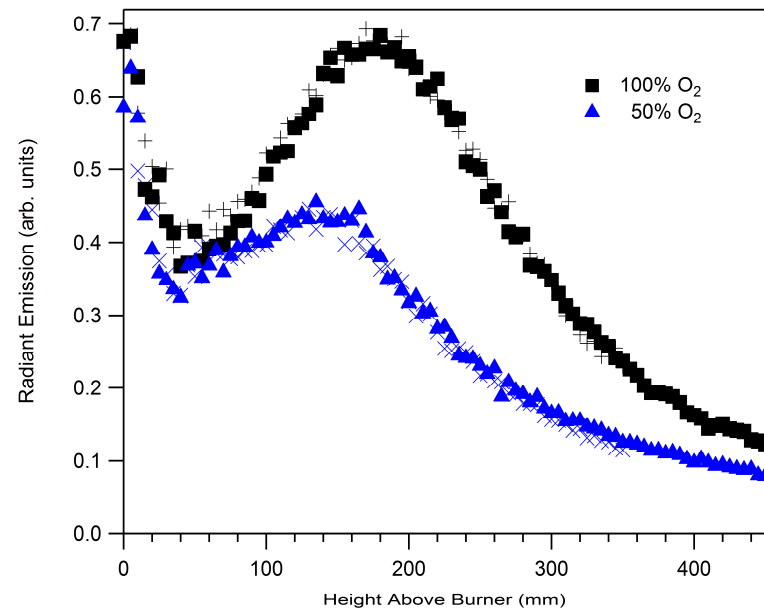
50% O₂ in N₂



100% O₂

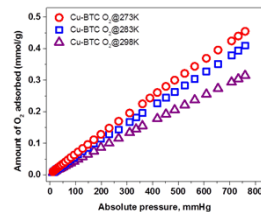
Radiant emission measurements have been performed along the flame centerline

- Data for 100% O₂ shows significantly more thermal radiation
- Flame temperatures are higher when using pure O₂ (more radiation from flame products)
- Some soot is formed in the 100% O₂ flame

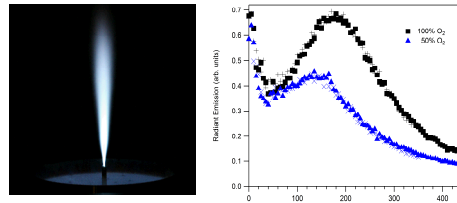


Systems Analysis of MOF-based Air Separation

MOF adsorption
isotherms (N₂ & O₂)
(from MOF team)



Optimal O₂:N₂ ratio
for combustion
(from combustion team)

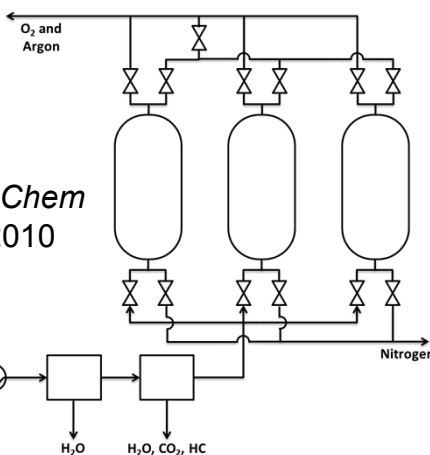


Can MOF-based
PSA reduce energy
consumption by 5%
vs. conventional PSA
air separation?

Construct and
validate model of
PSA process

Adjust PSA model
parameters to yield
desired O₂:N₂ ratio

Estimate energy
consumption based
on PSA parameters



Key PSA model parameters:

- Vessel dimensions
- Operating pressures
- Cycle time
- Feed rate

PSA energy consumption is
dominated by compressor(s)
→ Operating pressures and
flow rates are primary
drivers

Outline

- I. Nenoff Research Portfolio
- II. Metal-organic Frameworks (MOFs) for Separations
- III. O₂ separations for Oxyfuel Combustion
 - a. Introduction
 - b. Modeling
 - c. Metal-substituted MOFs
 - d. SMOF-7
 - e. Oxyfuel, combustion and techno-economic analysis
- IV. Conclusions and Future Work

IV. Conclusions and Future work

To Date: MOF Modeling (ab initio and MD Simulations) combined with Synthesis and Gas Sorption Testing, we identified and developed

- mixed metal MOFs for enhanced O₂ sorption over N₂ Co-, Fe- and Mn-analogues of Cu-BTC
- Novel MOFs (eg., SMOF-7) for enhanced O₂ separations

Future Direction: Process Development in which newly developed MOF materials replace zeolites in PSA processes for the energy efficient production of pure O₂ from air at temperatures up to ambient.

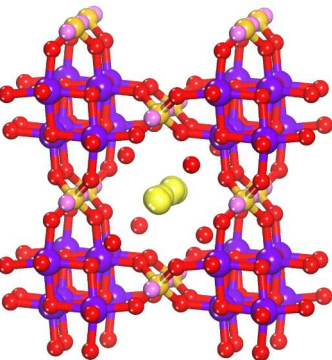
Target Results: Enhanced Energy Savings: up to 25%

Due to high selectivity and high capacity of the MOFs,
Plus increases in operating temperatures to near ambient

- Using previously studied/developed metal-organic frameworks (MOFs) tuned for O₂ selectivity
- Guided by techno-economic modeling
- Applied Energy R&D focus will be adsorption testing, primarily breakthrough systems up to ambient temperature
 - Complex gas stream mixtures of O₂, air, CO₂, Ar and H₂O
 - Development of cyclic adsorption processes

Sandia Research -> Technology

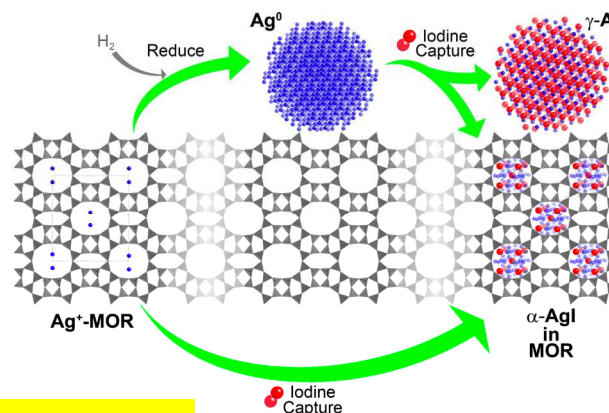
Environmental and Energy Applications



R&D 100 1996
JACerS, 2009, 92(9), 2144
JACerS, 2011, 94(9), 3053
Solvent Extr. & Ion Exch., 2012, 30, 33

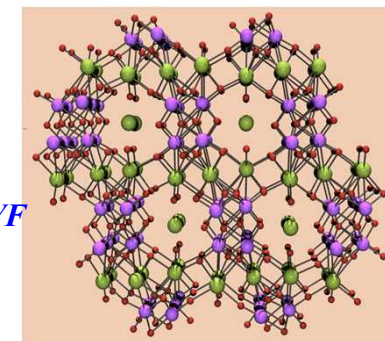
CST, Cs⁺ removal from water to Pollucite Waste Form
 US Patents 6,479,427; 6,110,378

I₂/ZIF-8, Isolation to Waste Form
JACS, 2011, 133(32), 12398
 US Patent filed 2012
JACS 2013, 135, 16256



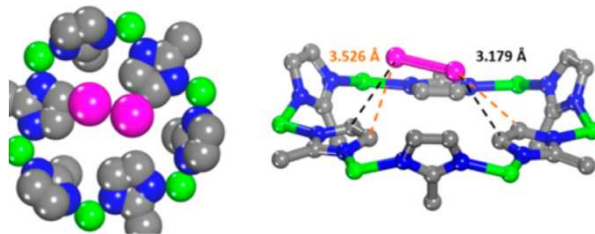
Ag-MOR
I₂(g) capture & mechanisms

JACS, 2010, 132(26), 8897
J Phys Chem Letters, 2011, 2, 2742

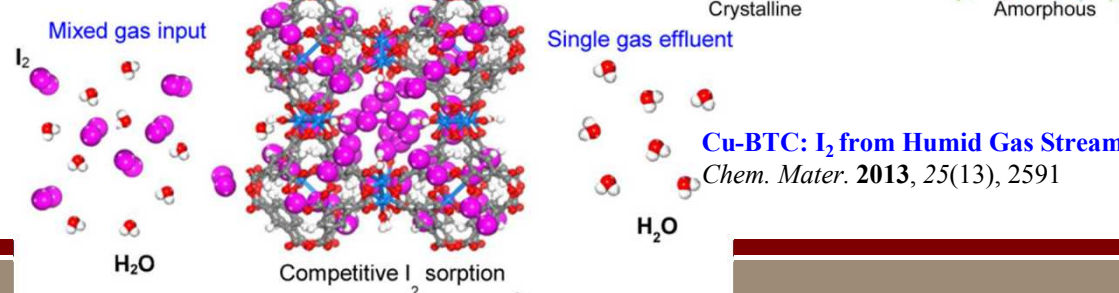
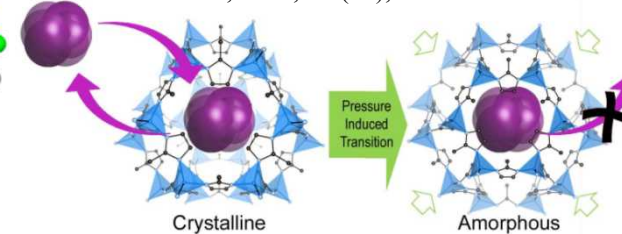


Fundamental Research to Applied to Commercial Products
Design the Separation Material To Develop the Waste Form

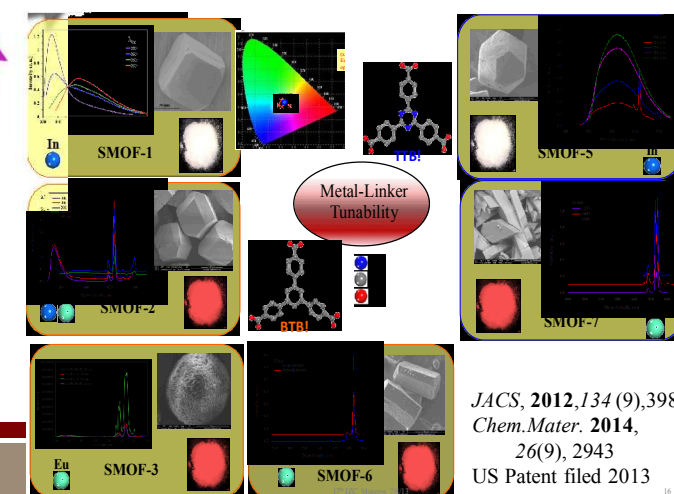
SOMS, Sr²⁺ getter, 1-step to Perovksite WF
JACS, 2002, 124(3), 1704
 US Patent 7,122,164



MOF Amorphization for Gas Storage
JACS, 2011, 133(46), 18583



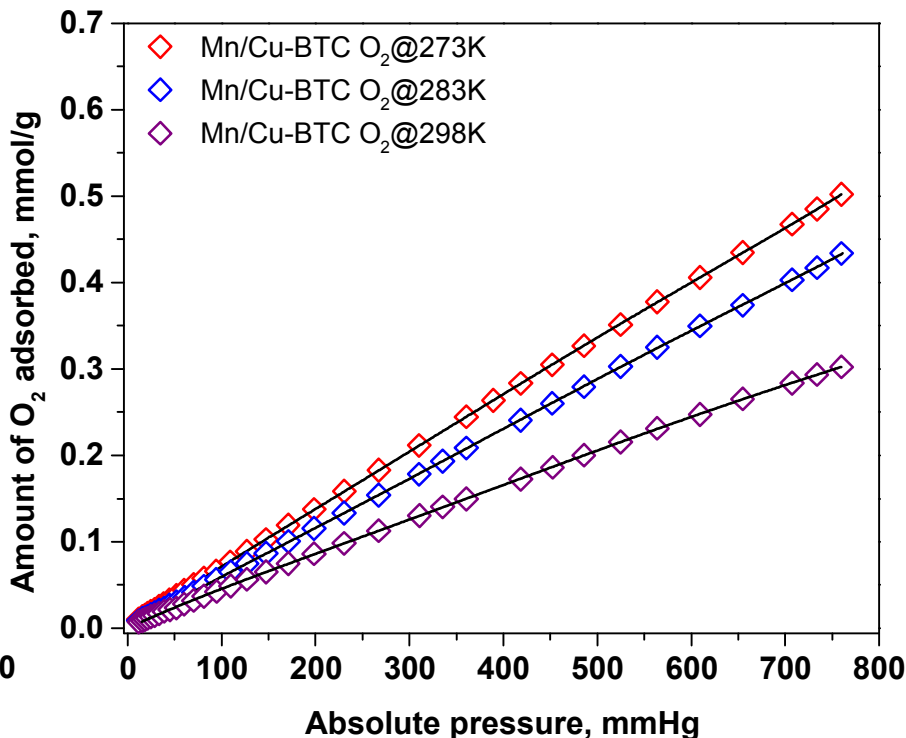
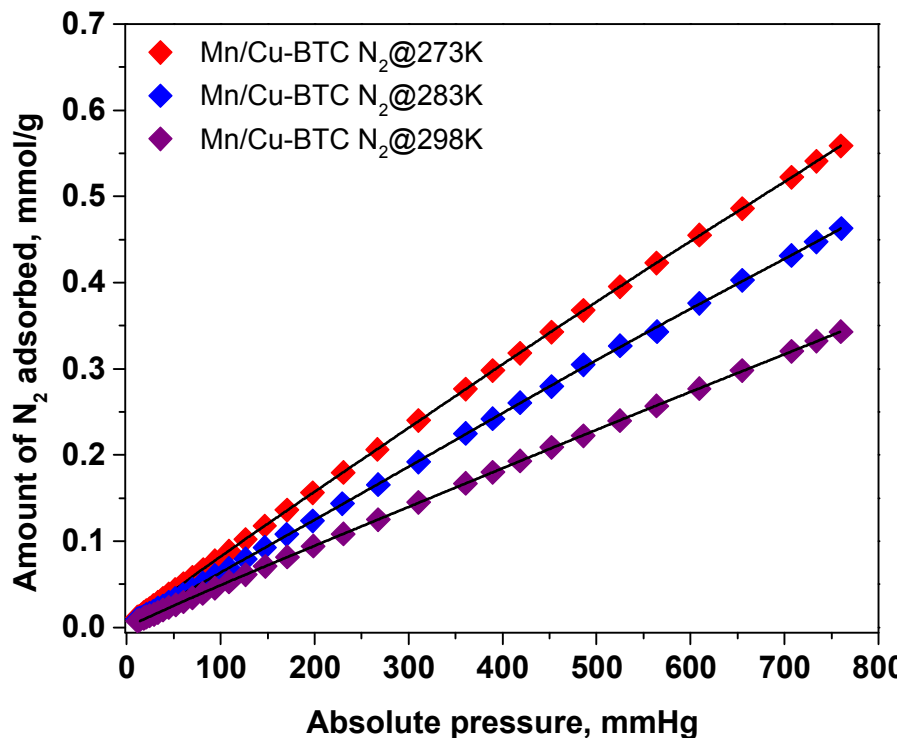
Cu-BTC: I₂ from Humid Gas Stream
Chem. Mater. 2013, 25(13), 2591



JACS, 2012, 134 (9), 3983
Chem. Mater. 2014, 26(9), 2943
 US Patent filed 2013

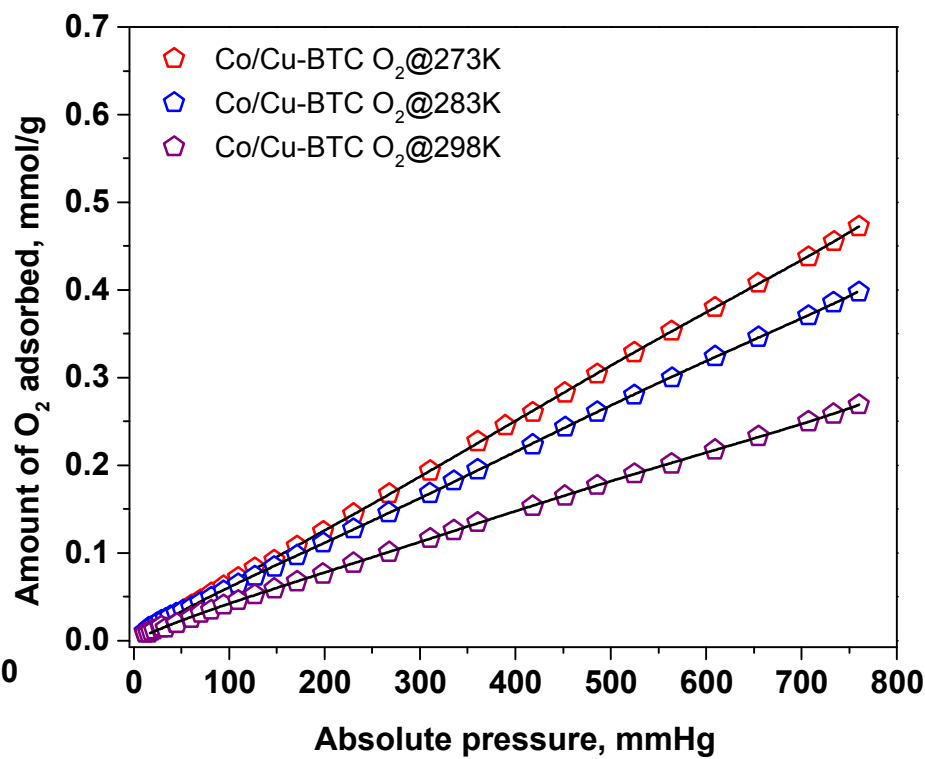
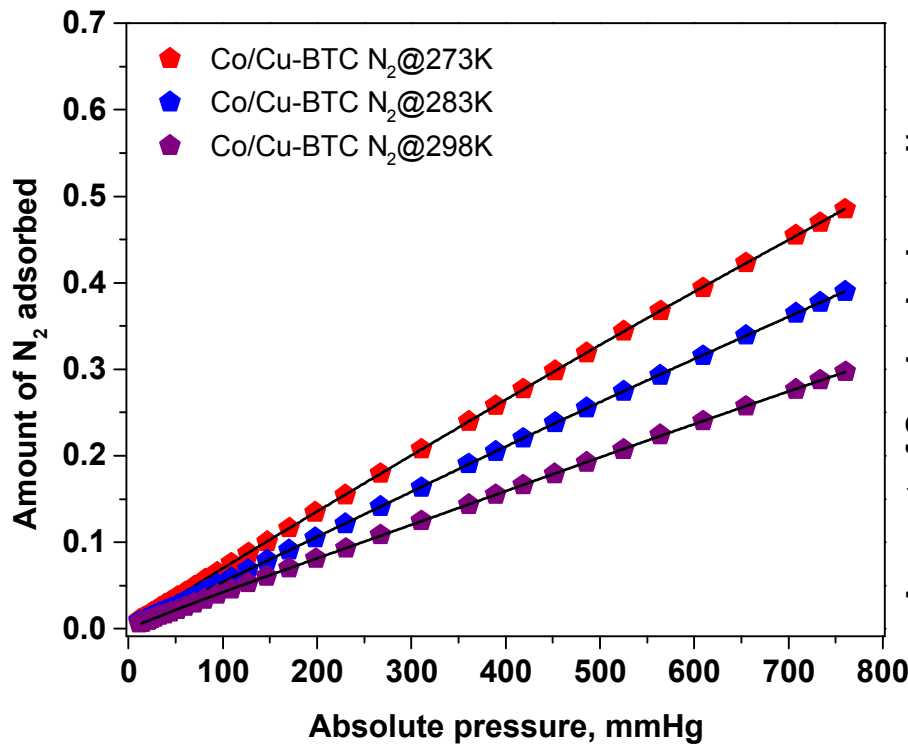
Thank You

N_2 and O_2 adsorption isotherms measured at 273, 283, and 298K on pristine Mn/Cu-BTC



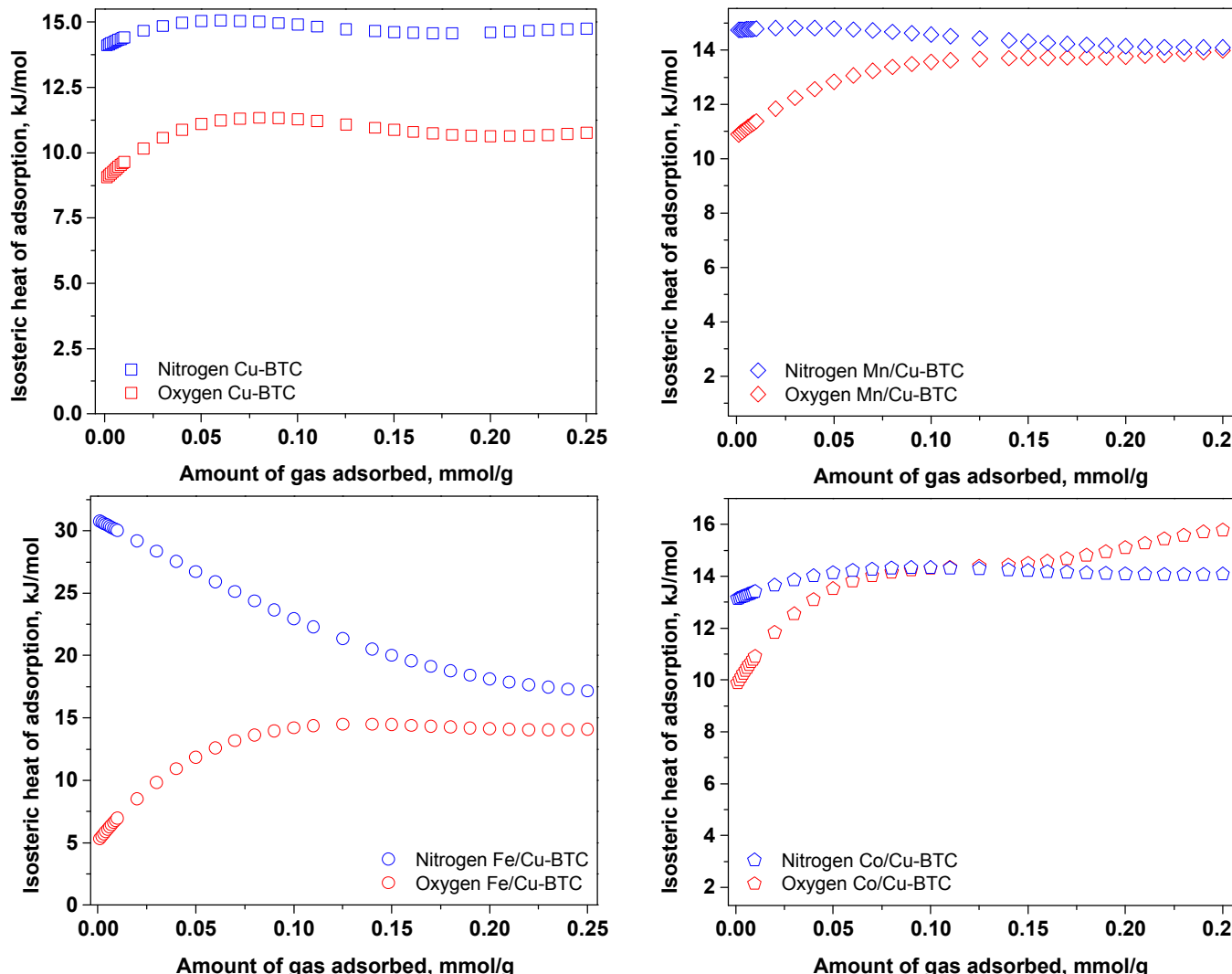
In the room temperature range, slightly higher affinity for N_2 over O_2 is noted

N_2 and O_2 adsorption isotherms measured at 273, 283, and 298K on pristine Co/Cu-BTC

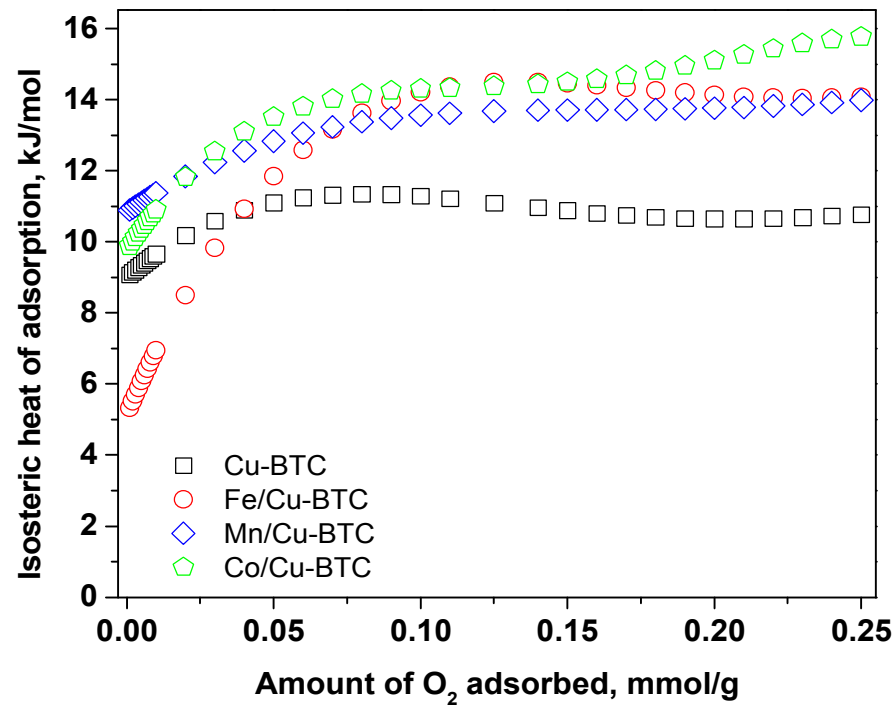
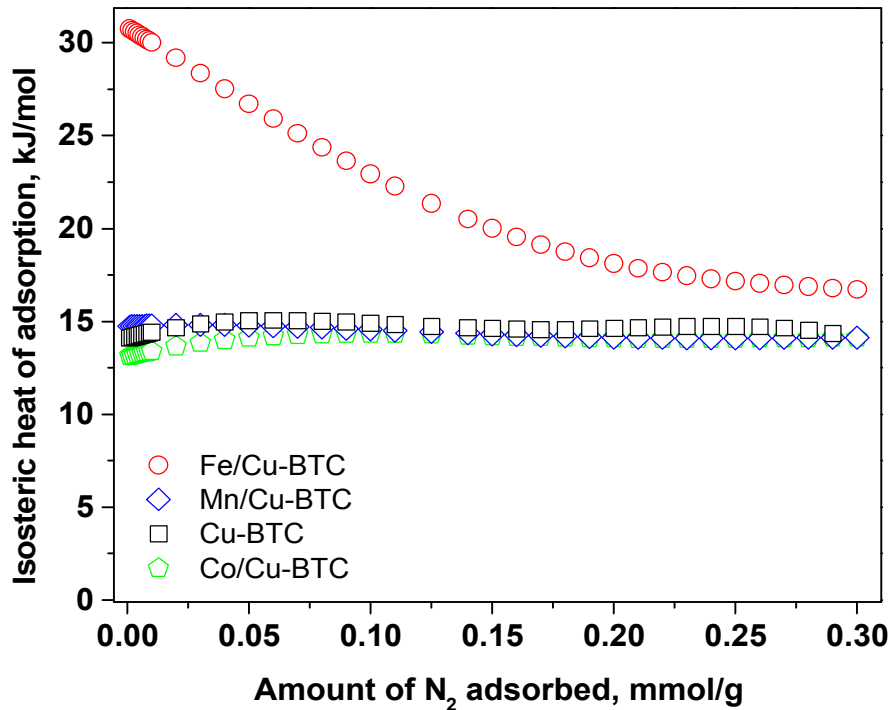


In the room temperature range, slightly higher affinity for N_2 over O_2 is noted

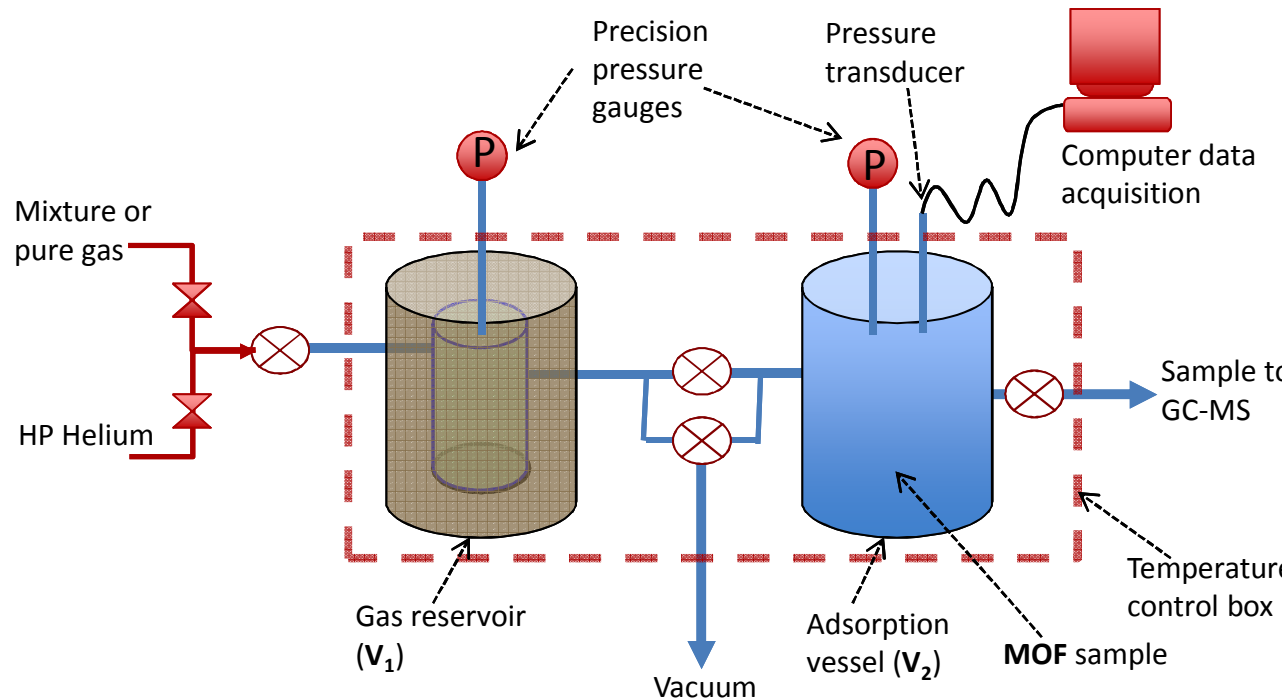
Significantly higher binding energy of N₂ over O₂ is noted for the Fe/Cu-BTC sample



Isosteric heats of adsorption for O₂ (red) and N₂ (blue) obtained from the fitted 273, 283 and 298K adsorption isotherms



O₂/N₂ Gas mixture adsorption measurements containing 20% O₂ and 80% N₂



Room temperature (294K) in pressure range of 1.77 to 5.2 bars.

Samples tested for adsorption of O₂/N₂ mixture containing 20% O₂ and 80% N₂ at 21, 35, and 48.5°C, respectively.

P_{eq} , bar	Amount adsorbed., cm ³ (STP).g ^{-1.bar⁻¹}		a_{O_2/N_2}
	O ₂	N ₂	
1.77	6.568	7.109	0.924
3.50	5.910	6.384	0.926
5.00	5.346	5.558	0.962

O₂ and N₂ binding energies trends across the first row transition metal series

